Numerical Simulation of the Spatial and Temporal Distribution of Sea Salt Particles on the Regional Scale

Degree project in Meteorology, 20p

KRISTINA LUNDGREN

Supervisors:
Bernhard Vogel, Karlsruhe University
Annica Ekman, Stockholm University

Department of Meteorology
Stockholm University
June 2006

Abstract

Sea salt particles have an impact on the global and regional climate by influencing factors such as atmospheric radiation, cloud formation and atmospheric heterogeneous chemistry. For this reason the aim of this study is to introduce a parameterization describing the emission of sea salt particles from the sea surface to the atmosphere for the regional atmospheric predicting model LM-ART. The particles are assumed to be emitted as dry particles and stay in this way during transport. The sea salt emission-parameterization is composed by three parameterizations describing the emission of particles with dry particle diameter D_p between 0.02 μm and 28 μm as a function of the 10-meter level wind speed and the sea surface temperature. It is seen that the amount of emitted particles with a dry particle diameter less than 1 μm increases with decreasing sea surface temperature while the opposite occurs for particles larger than 0.4 μm. The emission of sea salt particles increases with increasing wind speed. The large particles influence the total mass concentration the most, while the small particles have the largest influence on the total number concentration. For May 28-29th, 2005 3-D simulations over an area west of Ireland were performed examining the horizontal and vertical distribution of mass and number concentration of particles as function of temperature, wind speed and time. It is found that both number and mass concentration of sea salt particles are highly dependent on wind speed. Maximum reached mass concentration during this period is 300 μg m^{-3} and in number concentration 100 cm^{-3}. The maximum values both occur when the wind speed over the ocean is strongest. The transport over land is significant for the sea salt particles and it is found that the smallest particles dominate over larger particles over land since the number concentration is large also over land but the mass concentration decreases rapidly over land. Also the vertical mixing of sea salt particles is seen to be most effective for the smallest particles (in the sub micrometer size range). The differences in efficiency in transport of particles are mainly because of varying residence time in the troposphere, longer residence time for the smaller particles and shorter for the larger particles. Interaction with radiation, atmospheric chemistry or cloud processes are not taken into account in this work and will be the aim of future studies.

Table of Contents

1. Introduction

Sea salt particles affect the atmospheric radiation both directly by scattering incoming sunlight and indirectly through acting as cloud condensation nuclei and in this way help increasing the albedo of the marine boundary layer. They are important in heterogeneous chemical processes and for heat and moisture exchange between the sea surface and the atmosphere. The effects of sea salt aerosols will be further discussed in the following sections of the *Introduction.* However, shortly it can be concluded that sea salt particles have a great impact on the global and regional climate and are thus important constituents to consider in climate predicting models. In the future, the climate effect of sea salt particles is to be examined in the regional atmospheric predicting model LM-ART and the aim of this work is therefore to include sea salt particles in LM-ART.

1.1 Sea salt - an Important Troposheric Aerosol

The emissions of sea salt particles will remain regardless of anthropogenic activities since they are natural aerosols, which is one very important quality of these aerosols. Sea salt particles are primary marine aerosols, i.e. they are directly emitted to the atmosphere in comparison to secondary aerosol particles that are produced in the atmosphere by gas-to-particle conversion. Natural aerosols account for about 70 % of the total global aerosol loading (Satheesh and Krishna Moorthy [2005]) and sea salt is one of the absolutely most important components with a dominating aerosol mass component in marine air and sometimes also over land for remote regions. The production of sea salt aerosols is the strongest natural aerosol production with a general estimated global annual production of 1000-10.000 Tg Y^{-1}, which corresponds to about 35-70 % of all natural aerosols (Satheesh and Krishna Moorthy [2005]). According to IPCC (2001) the annual global emission of sea salt particles is 3340 Tg for the year 2000. The most important mechanism for production of sea salt aerosols is the wind action on the sea surface. This mechanism will be further discussed in Section 2.

Sea salt aerosols are important for heterogeneous chemical processes in the atmosphere, partly by providing a media for processes. The chemical composition of sea salt, based on the composition of seawater and ignoring atmospheric transformations, are according to Seinfeld and Pandis [1998] 55.04% Cl^-, 30.61% Na^+, 7.68% SO_4^{2-} and 6.67 % of other inorganic components. Since they are for example carriers of the chemical substances with Cl, Br, I and S they have big impact on the atmospheric cycle of those substances (Gong *et al*. [1997]). The components NaCl and NaBr of sea salt act as precursors to highly reactive chlorine and bromine atoms. These atoms may play a significant

role for ozone chemistry in the lower atmosphere (Finlayson-Pitts and Hemminger [2000]). The oxidation of SO_2 and NO_2 in marine boundary layers is also highly dependent on sea salt emissions (Finlayson-Pitts and Hemminger [2000], Foltescu *et al*. [2005]).

As mentioned above, sea salt particles furthermore have an effect on the exchange between the ocean surface and the atmosphere, for instance as they are important for heat and moisture transport (Foltescu *et al*. [2005]). According to Andreas [1998] the biggest particles, i.e. spume particles, probably are more important than the smaller bubble derived particles in transferring heat and moisture across the sea-air interface. Sea salt particles also have great radiative effects, which will be discussed in the next Section.

1.2 Radiative Effects

Sea salt particles affect the atmospheric radiation both directly and indirectly with dominating effects above ocean areas, mainly because of the relatively smaller concentration over land than over oceans. By scattering incoming sunlight the particles affect the radiation directly, whilst the indirect influences are due to sea salt particles acting as cloud condensation nuclei and thus help increasing the albedo of the marine boundary layer clouds. For a wind speed exceeding 12 m s^{-1}, sea salt can supply more than 80 % of the total cloud condensation nuclei for marine boundary layers, especially for winter seasons and high middle latitude regions (Foltescu *et al.* [2005]). O'Dowd and Smith [1993] concluded that under clean air and high wind conditions the sea salt aerosol can comprise the primary source for cloud condensation nuclei in stratiform clouds in maritime air. How the clouds in their hand play a role for the climate depends for instance on their vertical location and magnitude. According to Satheesh and Krishna Moorthy [2005] the direct radiative forcing of sea salt aerosols can be in the range of -0.5 to -2 W m^{-2} for low wind speeds, and can be as high as -1 to -6 W m^{-2} at higher wind speeds. Considering the predicted radiative forcing due to a future doubling of CO_2 which is about + 4 W m^{-2}, and the radiative forcing caused by increased CO_2 since the industrial era of about +1.5 W m^{-2}, the cooling effect of sea salt aerosol is obviously significant (Satheesh and Krishna Moorthy [2005]). Satheesh and Krishna Moorthy further concluded that the contribution to global radiative forcing of natural aerosols was important and that it was comparable or even larger to the direct radiative forcing of anthropogenic aerosols, which is estimated to be -0.4 Wm^{-2} for sulphate, -0.2 Wm^{-2} for biomass burning aerosols, -0.1 Wm^{-2} for fossil fuel organic carbon and +0.2 Wm^{-2} for fossil fuel black carbon aerosols (IPCC, 2001).

1.3 Transport and Sinks

Airborne sea salt particles are found in the size range of 0.02 μm to tenths of micrometers (Gong *et al*. [1997]). Large deposition and settling velocities give the biggest particles a short residence time in the atmosphere and for this reason they will not be transported to the upper troposphere. Hence, no long-range transport is likely for these particles. For the smallest particles the diffusivity is high and they are thus likely to be deposited on a pre-existing marine aerosol surface (Clarke *et al*. [2003]). The medium-size breaking-wave derived particles have a longer residence time in the atmosphere and therefore higher altitudes can be reached which makes participation in long-range transport possible. For the lowest atmospheric layer (0-200 m), Gong *et al*. [1997] found the mean residence time to range from up to 60 hours for small and medium-sized particles, with a dry particle diameter of D_P = 0.26-0.50 μm, down to 30 minutes for bigger particles, with a dry diameter D_P = 8-16 μm. The number distribution of sea salt particles is dominated by the sub micrometer size range, while the mass and volume distribution, which vary with the cubic of particle size, are dominated by the super micrometer size range.

Dry and wet depositions are the most important sink-processes for sea salt aerosols. According to Erickson and Duce [1988] the largest atmospheric sea salt deposition is found in the high latitude regions of both the Northern and the Southern Hemisphere. For sea salt particles the dry deposition globally dominates over wet deposition, but in areas associated with the Intertropical Convergence Zone, the airborne sea salt particles are removed efficiently by wet as well as dry deposition. Grini *et al*. [2002] found in their study that dry deposition was the dominating removal mechanism for sea salt particles in percent per mass.

According to the study by Grini *et al*. [2002] the largest concentrations of sea salt are found in areas with a large fraction of ocean and high wind speeds. High concentrations are therefore found for instance at mid-latitudes, particularly in the Southern Hemisphere. The largest production occurs, according to this paper, in January over Ireland. However in this area the dry and wet deposition are also high, so the resulting concentration is not the highest globally, but is still of the same order of magnitude as other areas with high concentrations. The mass concentrations of sea salt aerosols decrease with height. The transport of sea salt mass to higher altitudes in the troposphere is small and the sea salt aerosols that are transported to higher altitudes are removed by cloud and precipitation formation (wet deposition). No significant amount of sea salt can for this reason be found above the 750 hPa level (Grini *et al*. [2002]). Accordingly, the vertical profile of sea salt mass concentration

depends on efficiency in wet deposition but is also influenced by differences in transport and production. The global annual average burden of sea salt was found to be 12 mg m^{-2} by Grini *et al*. [2002], which they compared with earlier estimations between 7.5 and 36 mg m^{-2}. This value was also compared with the total burden of anthropogenic sulphate aerosols ranging from 1.7 to 3.6 mg m^{-2} and mineral dust that in two different data sets were estimated to be 35 and 110 mg m^{-2}, respectively.

Sea salt emissions and concentrations of sea salt particles are highly dependent on meteorology and have high spatial and temporal variability. The determination of the total size distribution of sea salt particles as function of wind speed is not an easy task. Small concentrations of the largest particles and the presence of sea salt aerosols in large size ranges contribute to this matter. Furthermore, measurements can only be made at specific locations and at certain times and to do measurements in conditions with high wind speeds are difficult. The correlation between local wind and sea salt mass concentration has been found to be poor, while the correlation between average wind and aerosol concentration is better observed. The reason of poor correlation between local wind speeds and sea salt mass concentration is probably due to advection from areas with high wind speeds to areas with low wind speeds (Satheesh and Krishna Moorthy [2005]).

1.4 Purpose

Since sea salt aerosols affect the atmospheric radiative balance and have an impact on the chemistry in the lower atmosphere, they also have an important impact on the regional and global climate. For this reason, a combination of three available parameterizations from the literature describing the sea salt emission flux is in this study included into a comprehensive regional-scale model system. The variation of sea salt aerosol flux given in number concentration and mass concentration, respectively, due to variations in parameters such as wind speed and temperature according to the chosen parameterizations is examined. It is also studied how the particles grow with relative humidity according to available parameterizations.

Furthermore, simulations of the flux of sea salt aerosols over the ocean west of Ireland are performed using data from the German Weather service for the periods of May 28-29th, 2005. The horizontal and vertical distribution of sea salt particles as a function of wind speed and sea surface temperature is studied. Only a few earlier works have simulated sea salt aerosol distribution as a function of water temperature, since there is only one recently proposed parameterization available to describe this

relationship. In addition, this work considers particles with dry diameters between 0.02 and 28 μm, i.e. a large fraction of the particles in the sub micrometer size range. This is also new compared to most earlier studies as parameterizations until a few years ago did not describe fluxes for particles with diameter less than one micrometer in a satisfying way.

2. Sea Salt Aerosol Production

The most important production mechanism of the sea salt aerosol is driven by the wind stress at the ocean surface. The so-called sea spray function describes how sea salt particles are emitted to the atmosphere from the sea surface. The emissions can be described as two different processes, sometimes referred as direct and indirect mechanisms, respectively. A schematic picture in FIGURE 2.1 describes them.

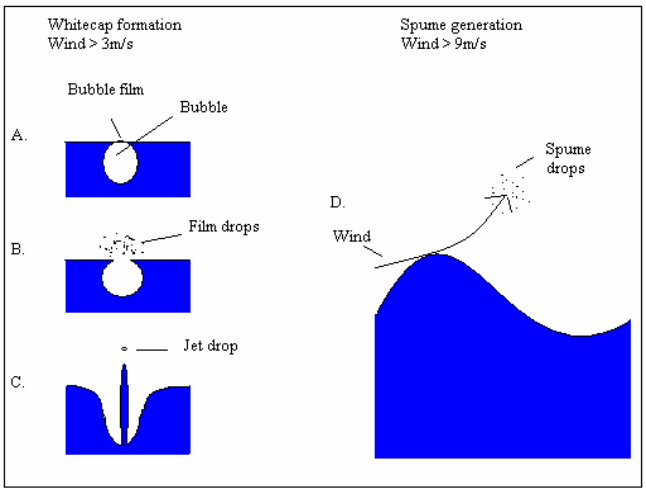

FIGURE 2.1. Sketch of the relevant sea salt aerosol production mechanisms for different wind regimes.

For wind speeds larger than approximately 3 m s^{-1} breaking waves, which are visualised as whitecaps, occur at the sea surface (Monahan and O'Muircheartaigh [1980]). The whitecap coverage increases with increasing wind speed and globally the average fraction of whitecaps is 1 % of the ocean surface (Mårtensson *et al*. [2003]). In breaking waves, air is mixed into the water and air bubbles are formed (FIGURE 2.1. Part A). When these air bubbles burst, the smallest sea spray droplets, film and jet drops, are emitted to the air in two different processes. Film drops are produced when the thin liquid film of the bubble ruptures and the remainder directly emitted vertically into the atmosphere (FIGURE 2.1. Part B.). After bubble bursting the remaining surface energy produces a vertical water jet that releases a so

called jet drop of sea salt into the atmosphere (FIGURE 2.1. Part C.). Film drops are dominated in the sub micrometer size range, with a dry median diameter of 0.2 μm while jet drops are found in the super micrometer size range with a dry median diameter of 2 μm according to observations by O'Dowd and Smith [1993]. It is thought that film drops dominate in number over jet drops for bubbles with diameter larger than 2 mm and that bubbles larger than 3.4 mm do not produce any jet drops (Mårtensson *et al*. [2003]). Bubbles, smaller than about 2 mm, do not form any film drops (Spiel [1998]). A maximum of 6 jet drops can be produced from every bubble while hundreds of film drops can be produced from each bubble, and the amount of film drops increase with the bubble diameter (Mårtensson *et al*. [2003]).

For greater wind speeds, higher than at least 9 m s^{-1} (Monahan *et al*. [1983]), the spume generation occurs. The spume droplets are the biggest sea spray droplets and are directly torn right off the wave crests by the wind (FIGURE 2.1. Part D). This formation of spume droplets can be called a direct mechanism and the generation of film and jet droplets can be called an indirect mechanism, due to the direct and indirect work, respectively, of the wind for the emission of sea salt to the atmosphere.

The sea salt particles are produced when the droplets evaporate completely. A salinity of 35 ‰ is typical for much of the world ocean. Over seawater, the corresponding equilibrium relative humidity is approximately 98 % (Lewis and Schwartz [2006]). This means that at the point of leaving the surface, the sea salt droplet has an ambient relative humidity of 98 %. Due to evaporation of the droplet the particle size at a relative humidity of 80 % is approximately half the size (Lewis and Schwartz [2006]). Being very hygroscopic because of the large fraction of sodium chloride sea salt absorbs water and the particle size increases as a function of ambient relative humidity and at the same time the particle density and refractive index are altered as more water is incorporated (Foltescu *et al*. [2005], Gong *et al.* [1997], Clarke *et al*. [2003]).

2.1 Parameterizations of the Sea Salt Aerosol Production

In this study, three different parameterizations describing the flux of sea salt particles from the sea surface to the atmosphere, in the size range of 0.02-28 μm dry particle diameter, have been utilized and will be described in this Section.

Although factors such as sea surface temperature and salinity do have an impact on the emissions of sea salt particles to the atmosphere (Mårtensson *et al*. [2003]), most functions describing the flux are based on solely wind speed and whitecap coverage. The dependence of oceanic whitecap coverage fraction W [%] as a function of wind speed U_{10} [m s^{-1}] at the 10-m level was described by Monahan and O'Muircheartaigh [1980] as following:

$$W = 3.84 \cdot 10^{-6} \cdot U_{10}^{3.41} \tag{2.1}$$

There are several available parameterizations describing the flux of sea salt particles from the sea surface to the atmosphere. Although it has been known for a long time that sea salt particles with dry particle diameter in the sub micrometer size range are emitted, many of those parameterizations are only valid for particles with diameters larger than 1 μm.

As mentioned before, the temperature of the sea surface is not included in most available parameterizations, although it is known that this parameter may influence the particle flux. At the moment the reasons for the temperature dependence can not be explained and needs further investigations. The parameterization of Mårtensson *et al.* [2003], is however partly empirically based on the water temperature and is moreover also valid for particles in the submicrometer size range with a dry particle diameter D_P down to 0.02 μm. The water temperature is derived by an approximation of the air temperature near the sea surface (Foltescu *et al*. [2005]). The parameterization of Mårtensson *et al*. [2003] describes the number of particles produced per second, logarithmic size increment and water surface area with bubbles:

$$\frac{dF_0}{d\log D_p} = \Phi W \qquad [\,m^{-2}s^{-1}\,] \tag{2.2}$$

where F_0 is aerosol number flux and W is the fraction of whitecap coverage in percent given in the whitecap cover equation (2.1). Φ describes the particle flux per whitecap area and is dependent on the water temperature T_w given in degrees Kelvin and the dry particle diameter D_p given in meters:

$$\begin{aligned} \Phi &= A_k T_w + B_k \\ A_k &= c_4 D_p^4 + c_3 D_p^3 + c_2 D_p^2 + c_1 D_p + c_0 \qquad k = 1,2,3 \\ B_k &= d_4 D_p^4 + d_3 D_p^3 + d_2 D_p^2 + d_1 D_p + d_0 \end{aligned} \tag{2.3}$$

k indicates three different size ranges and the coefficients $c_0 - c_4$ and $d_0 - d_4$ for each size range are given in TABLE 2.1.

TABLE 2.1. Coefficients for the three different size ranges *k* for the parameterization of A_k and B_k respectively in equation (2.3) according to Mårtensson *et al*. [2003].

	Size Interval [μm]	Coefficients				
		c_0	c_1	c_2	c_3	c_4
k=1	0.020-0.145	$-2.881 \cdot 10^{6}$	$-3.003 \cdot 10^{13}$	$-2.867 \cdot 10^{21}$	$5.932 \cdot 10^{28}$	$-2.576 \cdot 10^{35}$
k=2	0.145-0.419	$-6.743 \cdot 10^{6}$	$1.183 \cdot 10^{14}$	$-8.148 \cdot 10^{20}$	$2.404 \cdot 10^{27}$	$-2.452 \cdot 10^{33}$
k=3	0.419-2.800	$2.181 \cdot 10^{6}$	$-4.165 \cdot 10^{12}$	$3.132 \cdot 10^{18}$	$-9.841 \cdot 10^{23}$	$1.085 \cdot 10^{29}$
	Size Interval [μm]	Coefficients				
		d_0	d_1	d_2	d_3	d_4
k=1	0.020-0.145	$7.609 \cdot 10^{8}$	$1.829 \cdot 10^{16}$	$6.791 \cdot 10^{23}$	$-1.616 \cdot 10^{31}$	$7.188 \cdot 10^{37}$
k=2	0.145-0.419	$2.279 \cdot 10^{9}$	$-3.787 \cdot 10^{16}$	$2.528 \cdot 10^{23}$	$-7.310 \cdot 10^{29}$	$7.368 \cdot 10^{35}$
k=3	0.419-2.800	$-5.800 \cdot 10^{8}$	$1.105 \cdot 10^{15}$	$-8.297 \cdot 10^{20}$	$2.601 \cdot 10^{26}$	$-2.859 \cdot 10^{31}$

As a comparison, the source function of Monhanan *et al*. [1986] describes the number of particles produced per second, square meter area of bubbles and size increment given in micrometers for particles with a radius r_{80} in the size range 0.8-10 μm:

$$\frac{dF_0}{dr_{80}} = 1.373\ U_{10}^{3.41}\ r_{80}^{-3}\ \left(1 + 0.057\, r_{80}^{1.05}\right) \cdot 10^{1.19 e^{-B^2}} \qquad [\,m^{-2} s^{-1} \mu m^{-1}\,] \tag{2.4}$$

$$\text{Where } B = \frac{0.380 - \log r_{80}}{0.650}$$

U_{10} is the wind speed in m s^{-1} 10-meter level above the ground and r_{80} is the particles radius given in meter at the ambient relative humidity of 80 % and the validity range given above corresponds to the size interval 0.9-11.4 μm in dry diameter for the particle, D_p (Mårtensson *et al*. [2003]). Before the development of the described parameterization by Mårtensson *et al*. [2003], Eq. (2.2), available parameterizations for super-micrometer particles were sometimes extrapolated into smaller sizes. For instance, this commonly used parameterization of Monahan *et al*. [1986], Eq. (2.4), has been used for

smaller size ranges. It has though been shown that the function of Monahan *et al*. [1986] overestimates the flux of the smallest sea salt particles, which may have major consequences for calculations of the cloud condensation nuclei formation from sea salt aerosols (Mårtensson *et al*. [2003]) and for the calculation of the radiative effects.

Smith *et al*. [1993] used the measured number concentration N and the parameterized deposition velocity $v_{d_{SMITH}}$ to determine the variation of the flux of particles F with radius r using the following expression:

$$\frac{dF}{dr} = v_{d_{SMITH}} \frac{dN}{dr} \tag{2.5}$$

Based on the determined fluxes they came up with the following parameterization of the emission flux for particles with a radius r_{80} in 80 % relative humidity valid in the size range 1-25 μm, which corresponds to a dry particle diameter D_p of 1.1-28 μm. The flux is described in particles per surface area of bubbles, per second and size increment given in micrometers in the form of two log-normal distributions:

$$\frac{dF_0}{dr_{80}} = \sum_{i=1,2} A_i \exp\left(-f_i \left(\ln \frac{r_{80}}{r_{0i}} \right)^2 \right) \qquad [\, m^{-2} s^{-1} \mu m^{-1} \,] \tag{2.6}$$

r_{80} is the radius of the particle at an ambient relative humidity of 80 % given in micrometers and the constants have the values: $f_1 = 3.1\,\mu m$ $r_{01} = 2.1\,\mu m$, $f_2 = 3.3\,\mu m$ $r_{02} = 9.2\,\mu m$

The constants f_i and r_i remain unchanged with the wind speed while the coefficients A_1 and A_2 are strongly dependent on the wind:

$$\log A_1 = 0.676 \cdot U + 2.43$$

$$\log A_2 = 0.959 \cdot U^{0.5} - 1.476$$

There is also a modified version of the function of Smith *et al*. [1993] available (Hoppel *et al.* [2002], Glantz *et al*. [2004]).

$$\frac{dF_0}{dr_{80}} = \left[\frac{1}{v_{d_{SMITH}}} \left(\frac{dF_0}{dr_{80}} \right)_{SMITH} \right] \cdot v_d \tag{2.7}$$

Where $v_{d_{SMITH}}$ is the deposition velocity used by Smith *et al*. [1993] in equation (2.5) and v_d is a modified deposition velocity. In this work it is assumed that the factor of difference between the Eq. (2.6) of Smith and the version by Hoppel *et al.,* Eq. (2.7), with the modified deposition velocity is so small that it can be neglected. The function of Smith, Eq. (2.6), is used.

In this work the parameterizations (2.2), (2.4) and (2.6) are used to calculate the number emission of the sea salt particles. For simplification, it is assumed in the present work, that all sea salt particles are emitted to the atmosphere as dry particles and that they remain in that state during the whole model simulation. The time required for achieving chemical equilibrium with the surrounding is for small particles (with a diameter less then about one micrometer) of the order of one second and for the biggest particles a few minutes. Thus this is a fast process and for this reason it is assumed that the chemical composition and size of the particles are constant. This means that the parameterizations (2.4) and (2.6) had to be transformed from an expression describing the flux as a function of the humid particle radius to the same form as parameterization (2.2), i.e. into the form dF/dlogDp. This was done by using the relationship between humid particle radius and dry particle radius of Lewis and Schwartz [2006], Eq. (2.10), which will be described further in Section 2.2.

In FIGURE 2.2 the parameterizations used in this work are given in for their valid size intervals.

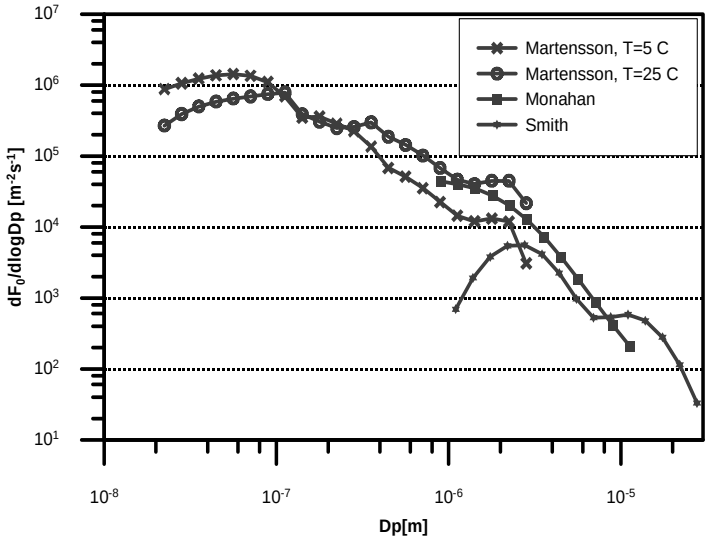

FIGURE 2.2. Parameterizations describing particle flux for particles with dry particle diameter from 0.02 μm to 28 μm for U_{10} = 9 m s^{-1}. Parameterization of Mårtensson et al. [2003] is described for two different sea surface temperatures, T_w = 25 °C and 5 °C.

The parameterization of Mårtensson *et al*. [2003] is chosen for particles with a dry particle diameter 0.02 μm<D_P<1 μm. For 1 μm<D_P<9 μm, the parameterization of Monahan *et al*. [1986] is used and the parameterization of Smith *et al*. [1993] is used to describe the flux of particles for particles 9 μm<D_P<28 μm. This is illustrated in FIGURE 2.3.

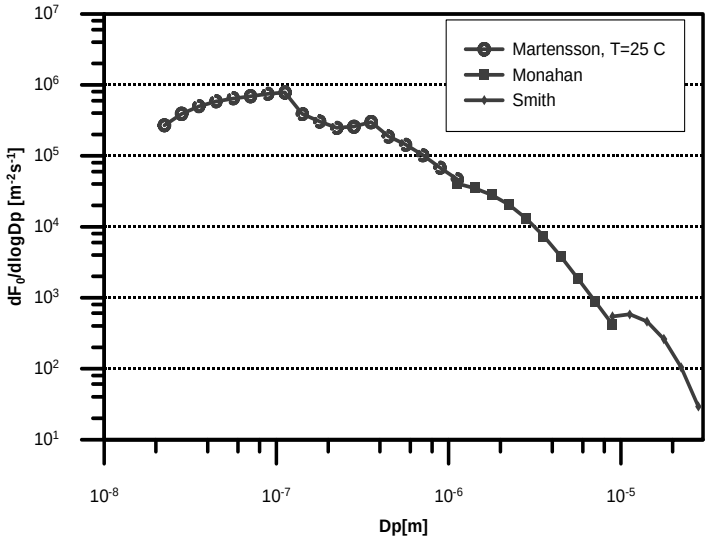

FIGURE 2.3. The three parameterizations describing flux of particles per area of bubbles and second for chosen intervals.

The flux $dF_0/d\log D_p$ of each particle size D_p given in meters is described in FIGURE 2.3. The total number concentration of sea salt particles is therefore achieved by performing a numerical integration:

$$E_N = \int_a^b \frac{dF_0}{d\log D_p} d\log D_p = \lim_{n\to\infty} \sum_{i=1}^{n} \frac{dF_0}{d\log D_p} \cdot \left(\Delta \log D_p\right) \qquad (2.8)$$

The integration is performed from the smallest particle diameter 0.02 μm to 28 μm with the constant step $\Delta \log D_p = 0.1$.

Following the approach of O'Dowd *et al*. [1997], it is assumed that each one of the three sea spray mechanisms for film drops, jet drops and spume drops, described in the beginning of Section 2, corresponds to a log-normal distribution. The diameter for each mode is $D_{m,i}$ given in meters with the corresponding standard deviation σ_i so that a tri modal log-normal curve can describe the measurements of number concentration of the particles. The values of the parameters described in TABLE 2.2 are used:

TABLE 2.2. Particle mode diameter D_m [m] for the film , jet and spume mode and corresponding standard deviation.

Particle Size Mode	Mode Diameter [m]	Standard deviation
Film	$0.2 \cdot 10^{-6}$	1.9
Jet	$2 \cdot 10^{-6}$	2
Spume	$12 \cdot 10^{-6}$	3

From the number flux E_N, the mass flux E_m was calculated by using the following relation:

$$E_{m,i} = \frac{\pi \cdot \rho_p \cdot D_{m,i}^3}{6} \cdot \exp\left(\frac{9}{2} \cdot (\ln\sigma_i)^2\right) \cdot E_{N,i} \qquad i=1,2,3 \qquad (2.9)$$

The values used for the median dry particle diameter $D_{m,i}$ and belonging standard deviation σ_i for the three modes *i* identified as film, jet and spume droplets according to O'Dowd *et al.* [1997] respectively are given in TABLE 2.2.

2.2 Relation between Humid- and Dry Particle Sizes

The flux of sea salt particles is often described as a function of the particle radius in air with relative humidity of 80 %, r_{80}. However, the dry particle radius r_d or dry particle diameter D_p is sometimes used instead.

The three parameterizations that are used in this work are given for different types of particle sizes, based on both humid and dry particle radius/diameter. To transform the flux described for a radius in a certain relative humidity to a flux as a function of the dry particle size there are a few parameterizations available in the literature. Lewis and Schwartz [2006] describe the relationship between the dry particle radius and the radius at a relative humidity RH as:

$$r_{RH} = (r_d)\left(\frac{4.0}{3.7}\right)\left(\frac{2.0 - RH}{1 - RH}\right)^{\frac{1}{3}} \tag{2.10}$$

Where the dry radius have been define as $r_d = \left(\frac{3m_d}{4\pi\rho_S}\right)^{\frac{1}{3}}$

With m_d as the mass of dry sea salt in the particle

and $\rho_S \approx 2.2\ g\,cm^{-3}$ as the density of dry sea salt.

FIGURE 2.4 illustrates the particle growth as function of ambient relative humidity according to the parameterization of Lewis and Schwartz [2006]. The dry particle size was assumed to be 1 μm in diameter, i.e. 0.5 μm dry particle radius, and from this value the corresponding humid radius was calculated for 0.4 <RH< 1.

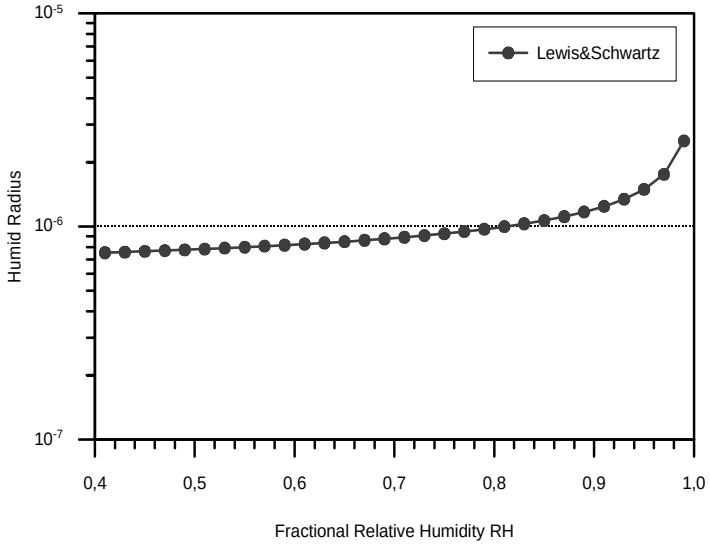

FIGURE 2.4. From a dry particle radius of 0.5 μm the humid particle radius is calculated as function of relative humidity by using the parameterization of Lewis and Schwartz [2006], Eq. (2.8).

The particle grows with increasing relative humidity (FIGURE 2.4), and the rate of growth increases with increasing relative humidity. At a relative humidity of 98 % the parameterization of Lewis and Schwartz (Eq. 2.10) is $r_{98} = 2.00$ μm and at 80 % the radius is $r_{80} = 0.98$ μm. The fraction r_{98} / r_{80} is 2.04. According to the literature the size at 80 % relative humidity is approximately half of the size at formation, which can be referred to the size at relative humidity of 98 % (Lewis and Schwartz [2006]). In Lewis and Schwartz [2006] several parameterisations are studied and they all give the fraction value of 2.

3. Sensitivity Studies

As described in Section 2.1 three parameterizations, Eqs. (2.2), (2.4) and (2.6), are used in this work to describe the emission of sea salt particles to the atmosphere. In this section those parameterizations are studied for changes in wind speed and sea surface temperature (the latter only possible for the parameterization Mårtensson *et al*. [2003], Eq. (2.2)). The changes in number and mass density fluxes are studied separately.

3.1 Number Density Flux

Changes in water temperature and wind speed affect the particle flux of the smallest particles according to Mårtensson *et al*. [2003]. As can be seen in FIGURE 3.1, the flux of particles, according to Eq. (2.2), with diameter D_P<0.1 μm increases with decreasing temperature while the opposite occurs for particles with D_P>0.4 μm. Between 0.1 μm and 0.4 μm no clear trend can bee seen with changes in water temperature. The size dependence of the flux is similar for all temperatures for particles with D_P>0.4 μm whilst a clear change of the curves shape can bee seen for the particles with dry diameter less than 0.1 μm, where the maximum flux occurs for bigger particles with increasing temperature.

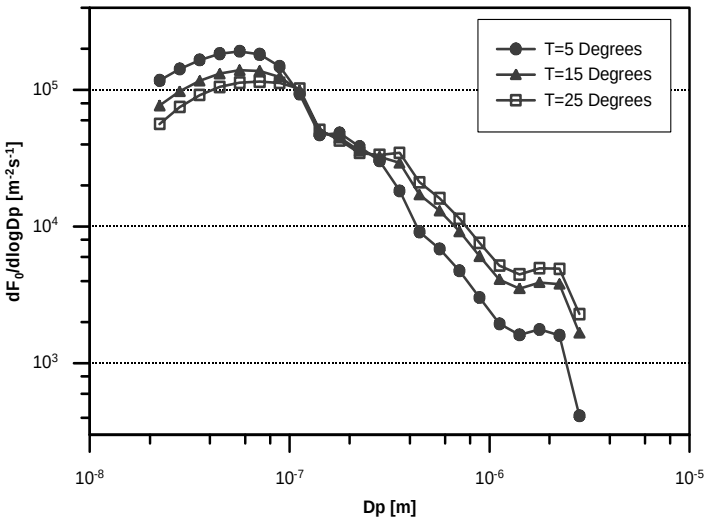

FIGURE 3.1. Mårtensson *et al*. [2003] parameterization, Eq. (2.2) describing particle flux for wind speed U_{10} = 5 m s^{-1} and different water temperatures.

Integrations of the fluxes in FIGURE 3.1 over the corresponding particle size interval show that the total amount of particles emitted to the atmosphere increases with decreasing temperature at a certain wind speed.

The particle fluxes according to Mårtensson *et al*. [2003], Eq. (2.2), are calculated for a fixed sea surface temperature to see the dependence of the fluxes with changes in wind speed. In FIGURE 3.2 the result is shown for a water temperature of 15 °C.

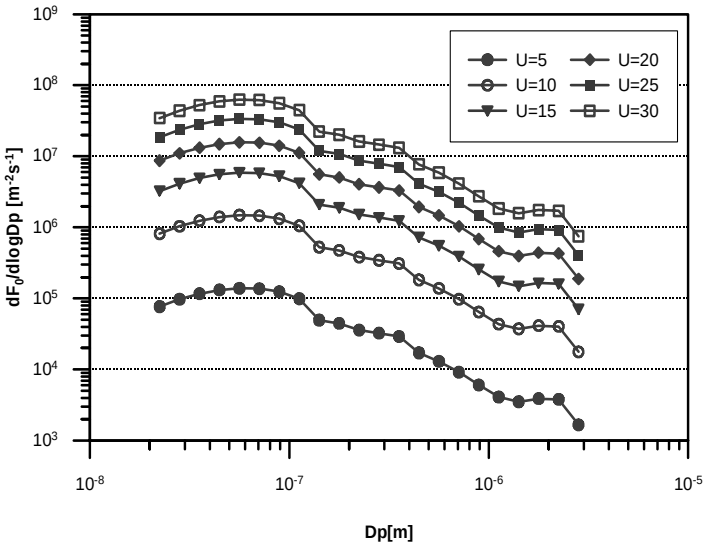

FIGURE 3.2. Particle flux according to Mårtensson *et al.* [2003], Eq. (2.2), for different wind speeds [m s^{-1}] but constant water temperature at 15 °C.

For all temperatures the particle flux increases with increasing wind speed. The flux of particles increases most quickly with an increase of the wind at low wind speeds.

The dependence of the flux of particles on wind speed according to Monahan *et al.* [1986], Eq. (2.4), is shown in FIGURE 3.3.

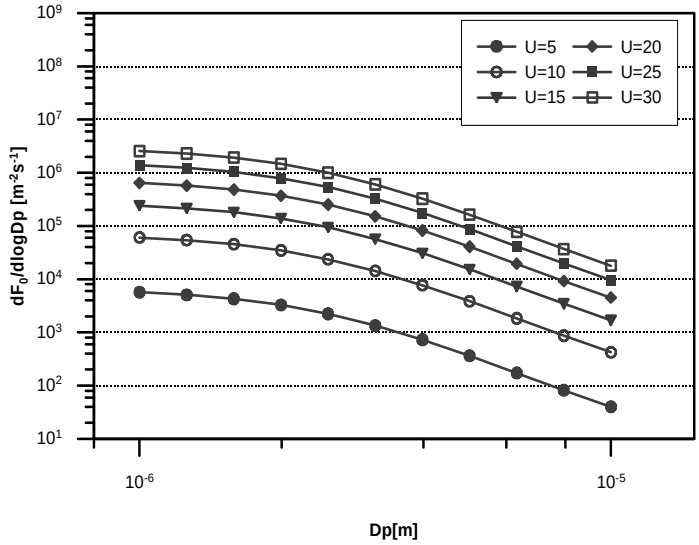

FIGURE 3.3. The parameterization of Monahan *et al.* [1986], Eq. (2.4), for different wind speeds [m s^{-1}].

It can be seen that the flux of particles increase with wind speed and that the increase is fastest for increases in low wind speeds.

In FIGURE 3.4 the results from calculations of the particle flux using parameterization of Smith *et al*. [1993], Eq. (2.6), for increasing wind speeds are presented.

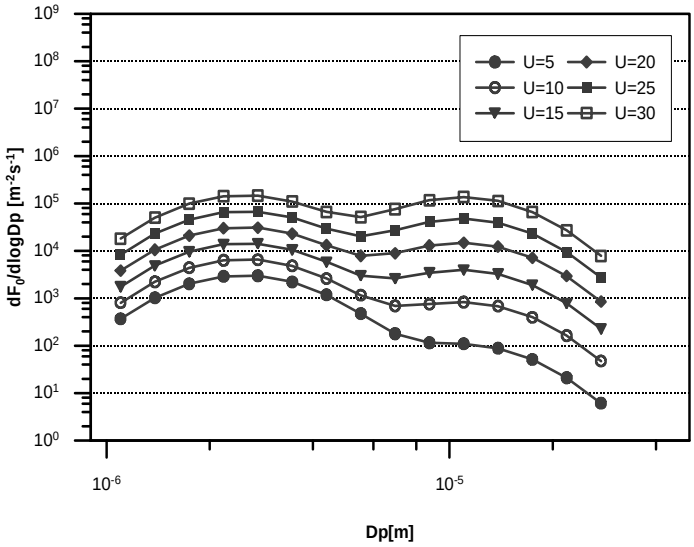

FIGURE 3.4. The parameterization of Smith *et al.* [1993], Eq. (2.6) describing the number concentration for different wind speeds [m s^{-1}].

As mentioned before the function of Smith *et al*. [1993] contains two log-normal distributions, which here also can be seen. With increasing wind speed increases the amount of particles emitted from the sea surface to the atmosphere. For a wind speed higher than 9 m s^{-1} the increase of amount of particles emitted described by the log-normal distribution centred at about 10 μm increases more rapidly with wind speed than the amount of smaller particles. According to Andreas [1998] the minimum diameter of spume droplets are generally about 10 μm, which are only generated for wind speeds higher than 9 m s^{-1}. The illustration of the parameterization of Smith *et al*. [1993] in FIGURE 3.4 can therefore be concluded to describe the effect to the number concentration of the spume particle generation.

The amount of particles is seen to increase with increasing wind speed for all three parameterizations. Changes at low wind speed convey to changes in the number concentration of the particles more quickly than changes at high wind speed. The amount of particles emitted is for all wind speeds

highest for the smallest particles (FIGURE 3.2) and smallest for the biggest particles (FIGURE 3.4). The biggest difference between the utilized parameterizations is that the temperature effect as mentioned only can be studied for the parameterization of Mårtensson *et al*. [2003] describing the flux of the smallest particles (Eq. (2.2)).

3.2 Mass Density Flux

From the number density flux of the small (*film drops*), medium-sized (*jet drops*) and large particles (*spume drops*), respectively, the mass density flux of each of these modes is calculated according to Eq. (2.9). The mass density fluxes are calculated for different wind speeds. When the total mass density flux of those three size modes together is calculated it is obvious that the total mass concentration is approximately equal to the mass concentration of the larges particle mode for each wind speed. The influence of the two smallest size modes do not contribute to the total mass concentration and are therefore not illustrated here. The change of the total mass flux and the mass flux of the large sea salt particles with increasing wind speed is illustrated in FIGURE 3.5.

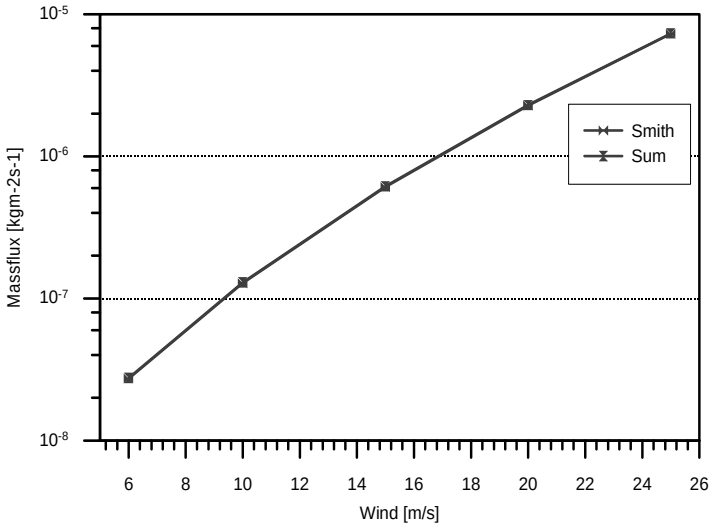

FIGURE 3.5. Dependence of total mass flux and mass flux for the largest particle sizes, calculated according to Smith *et al.* [1993].

The mass flux summarized over the whole particle size interval of 0.02-28 μm is compared to the mass flux for the largest particles, i.e. the spume mode here referred to as the particles with a dry diameter between 9-28 μm. Increasing wind speed results in higher mass flux with an exponential dependence of mass flux on the wind speed.

For a wind speed of 6 m s^{-1}, which according to measurements is about the global annual average wind speed above the ocean at 10-m level (Archer and Jacobson [2005]), the total global mass flux was calculated to be about $2.77 \cdot 10^{-8}$ kg m^{-2} s^{-1}. Assuming that 1% of the global ocean coverage is covered by whitecaps this mass flux corresponds to a global annual flux of approximately 3200 Tg Y^{-1}. This number is comparable to the estimated emission of 3340 Tg Y^{-1} according to IPCC, 2001.

4. Model Description

In this study the model system LM-ART is used to simulate regional distribution of sea salt particles. ART stands for **A**erosols and **R**eactive **T**race gases and LM (***L**okal-**M**odell*) is a nonhydrostatic limited-area atmospheric prediction model developed by the German Weather Service (*Deutscher Wetterdienst, DWD)*. In this report only a short description of the LM will be given, for a more detailed documentation cf. Doms and Schättler [2002]. The basic equations of LM based on the work by Doms and Schättler [2002] are summarized in Appendix A.

The combined model system LM-ART was developed at the Institute of Meteorology and Climate Research at the University of Karlsruhe, Germany. FIGURE 4.1 gives an overview of the model system LM-ART where the individual model components and necessary input data are shown. The green boxes indicate those modules where sources and sinks are treated. The blue boxes mark those modules where atmospheric physical and chemical processes and the aerosol dynamics are handled. The orange coloured boxes indicate additional external input data, which are necessary for conducting a model run. The whole system runs in an online-coupled model frame with time steps of the order of tenth of seconds.

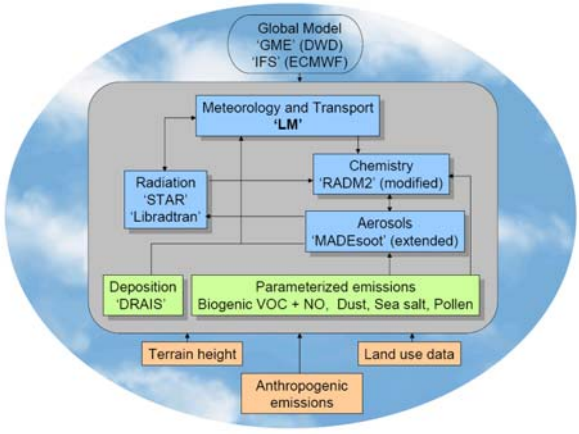

FIGURE 4.1. Schematic sketch of the model system LM-ART.

The initial and boundary conditions can be provided by the Global Model (GME) of the German Weather Service (DWD) or from the global model IFS of ECMWF. Necessary input data are the height of the terrain, anthropogenic emissions and land use data. Emission parameterizations of particles of mineral dust, pollen, bacteria are already included in the model system. In this work sea salt is included as a new particle class. The emitted particles are included in the modal aerosol model MADEsoot (Riemer *et al*. [2003]) and influenced by meteorology and transport in LM, by chemistry in RADM2, radiation in STAR or Libradtran and deposition in DRAIS.

LM-ART will in the near future be used to perform operational pollen predictions based on numerical simulations, to quantify feedback processes between aerosols and the state of the atmosphere and to quantify the interaction between trace gases and aerosols on the regional scale. Parameterizations to simulate the interactions between aerosols and radiation and the feedback of this process with the atmospheric variables are under development. LM-ART will also be used for parameterizations of feedback processes between aerosols and the state of the atmosphere and interaction between trace gases and aerosols for larger scale models.

4.1 The Treatment of Sea Salt in LM-ART

In order to take into account the size distributions of the particles the log-normal approximation is applied. Three modes are used to describe the sea salt particles, where the standard deviation is kept constant for each mode. Then the number density and the mass density of each mode are handled as additional tracers.

4.2 Size Distribution of Number and Mass Density

The number and mass concentrations of sea salt particles are assumed to be log-normal distributions.

The number distribution is given by:

$$n_i\left(\ln D_p\right) = \frac{N_i}{\sqrt{2\cdot\pi}\cdot\ln\sigma_i}\cdot\exp\left(-\frac{\left(\ln D_p - \ln D_{g,i}\right)^2}{2\cdot\ln^2\sigma_i}\right) \qquad i=1,2,3 \qquad (4.1)$$

And the mass distribution is in the corresponding way given by:

$$m_i^*(\ln D_p) = \frac{m_i}{\sqrt{2\cdot\pi}\cdot\ln\sigma_i}\cdot\exp\left(-\frac{\left(\ln D_p - \left(\ln D_{g,i} + 3\ln^2\sigma_i\right)^2\right)}{2\cdot\ln^2\sigma_i}\right) \qquad i=1,2,3 \qquad (4.2)$$

Where $D_{g,i}$ is the number median diameter, D_p is the dry particle diameter and σ_i is the geometric standard deviation, which is assumed to be constant for each mode. The values chosen for those variables are given in TABLE 2.2.

The median diameter of the log-normal distributions can vary with time and space and is determined from:

$$D_{g,i} = \sqrt[3]{\frac{m_i}{\frac{\pi}{6}\cdot\rho_s\cdot\exp\left(\frac{9}{2}\cdot\ln^2\sigma_i\right)\cdot\overline{N_i}}} \qquad i=1,2,3 \qquad (4.3)$$

with ρ_s as the bulk density of the sea salt particles.

In order to include sea salt as an additional component into the model system LM-ART the following simplifications are made. Coagulation, condensation and evaporation as well as chemical reactions are neglected. Wet deposition, which is an important sink for the sea salt particles, is also neglected. The inclusion of this important process will be a subject of future work. The equations that describe the transport the turbulent diffusion and the sedimentation of the total number and the total mass density are then given by:

$$\rho\frac{dq^{N_i}}{dt} = -\nabla\cdot\left(P^{N_i} + F^{N_i}\right)$$

$$\rho\frac{dq^{m_i}}{dt} = -\nabla\cdot\left(P^{m_i} + F^{m_i}\right) \qquad i = 1,2,3 \qquad (4.4)$$

with

$$q^{N_i} = \frac{N_i}{N}$$
$$q^{m_i} = \frac{m_i}{\rho} \qquad i = 1,2,3 \qquad (4.5)$$

N is the total number of particles per m^{-3} including the air molecules.

The sedimentation fluxes are given by:

$$P^{N_i} = \rho q^{N_i} v_{s,N_i}$$
$$P^{m_i} = \rho q^{m_i} v_{s,m_i} \qquad i = 1,2,3 \qquad (4.6)$$

where v_{s,N_i} and v_{s,m_i} are the sedimentation velocities of the number and the mass density, respectively.

4.3 The Sedimentation Velocities

The sedimentation velocities for the number and the mass density are given by Stokes Law with Cunningham slip correction for the smallest particles, integrated over the log-normal distribution (Kramm *et al.* [1992], Binowski and Shankar [1995] and references therein):

$$v_{sN,i} = \frac{g \cdot \rho_p}{18 \cdot \nu \cdot \rho_a} \cdot \left[\exp\left(2 \cdot \ln^2 \sigma_i\right) + 1.246 \cdot \frac{2 \cdot \lambda_a}{D_{g,i}} \cdot \exp\left(\frac{1}{2} \cdot \ln^2 \sigma_i\right) \right] \qquad i = 1,2,3 \qquad (4.7)$$

$$v_{s,m_i} = \frac{g \cdot \rho_p}{18 \cdot \nu \cdot \rho_a} \cdot \left[\exp\left(8 \cdot \ln^2 \sigma_i\right) + 1.246 \cdot \frac{2 \cdot \lambda_a}{D_{g,i}} \cdot \exp\left(\frac{7}{2} \cdot \ln^2 \sigma_i\right) \right] \qquad i = 1,2,3 \qquad (4.8)$$

Where $D_{g,i}$ is determined from equation (4.3), ν denotes the kinematic viscosity of air and λ_a the mean free path of air.

4.4 Emissions

The emissions enter equations (4.4) via the lower boundary conditions. As described in Section 2.1 the parameterizations (2.2), (2.4) and (2.6) are used to calculate emissions of the number densities of the particles. Equation (2.4) and equation (2.6) are transformed into the form dF/dlogDp by using the relationship between humid radius and dry particle radius of Lewis and Schwartz [2006], Eq. (2.10). In this work the parameterization of Mårtensson *et al*. [2003] is chosen to describe the particle flux from the sea surface to the atmosphere for particles with dry particle diameter 0.02 μm<D_p<1 μm, here referred as the film mode. From 1μm up to 9μm, the jet mode, in dry particle diameter the parameterization of Monahan *et al*. [1986] is used and the parameterization of Smith *et al*. [1993] is used to describe the flux of particles for particles with a dry diameter 9 μm<Dp<28 μm, here referred as the spume mode. The total number concentration integrated over the whole size interval 0.02-28 μm, Eq.(2.8) and total mass concentration Eq. (2.9) are introduced into the model LM-ART.

5. 3-D Case Study: May 28-29th, 2005

In this section the chosen weather situation for the 3-dimensional simulation of sea salt number and mass concentration together with the results will be discussed. The model domain chosen for this work is illustrated in FIGURE 5.1. It extends from 7.880 W to 14.708 W and 49.383 N to 57.731 N and contains parts of Ireland. It includes one of the European Atmospheric Research Centres, which is situated in Mace Head (53, 19 N; 9, 54 W) on the west coast of Ireland. At this station aerosol measurements have been performed since 1958. In this region there is a high possibility of significant sea salt aerosol concentrations when the wind speeds are high enough. For strong westerly winds, transport of sea salt particles from the ocean to Mace Head and over Ireland is possible. Grini *et al.* [2002] simulated the global annual maximum of sea salt particle production in an area over the Atlantic Ocean, near Mace Head.

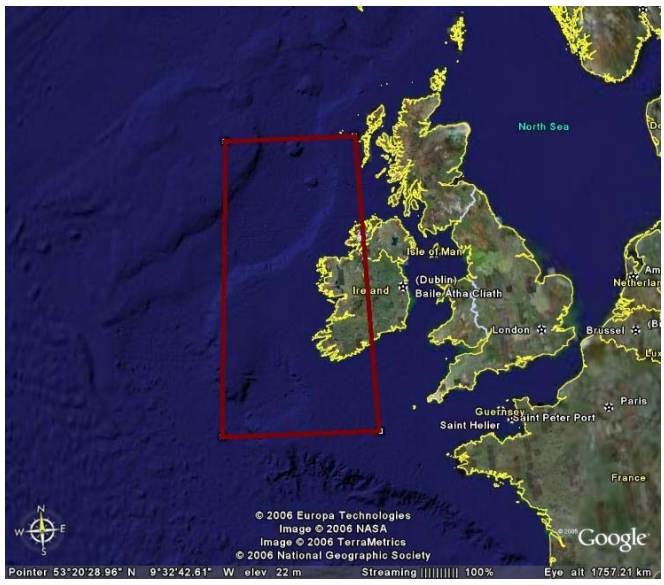

FIGURE 5.1. Illustration of region chosen for 3-D simulation of sea salt aerosol production.

The simulation is carried out for the period of May 28-29th of the year 2005. FIGURE 5.2 and FIGURE 5.3 illustrate the weather situation in Europe during this period of time.

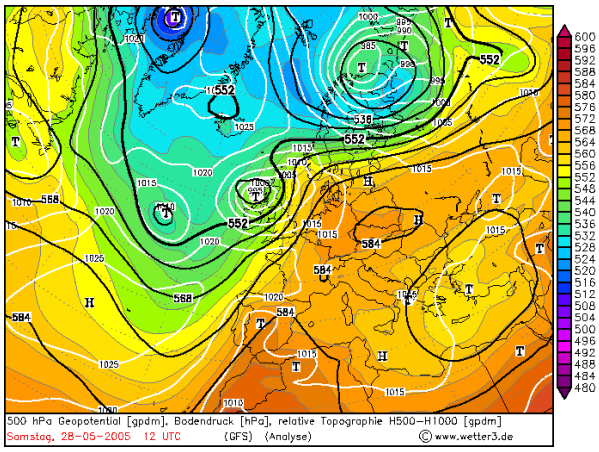

FIGURE 5.2 a) Mean sea level pressure [hPa] (white lines) at 12 UTC May 28th, 2005.

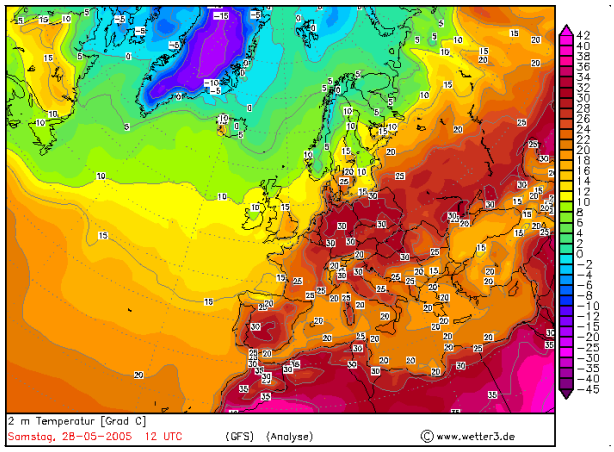

FIGURE 5.2 b) Temperature [°C] 2 meters above the ground at 12 UTC May 28th, 2005.

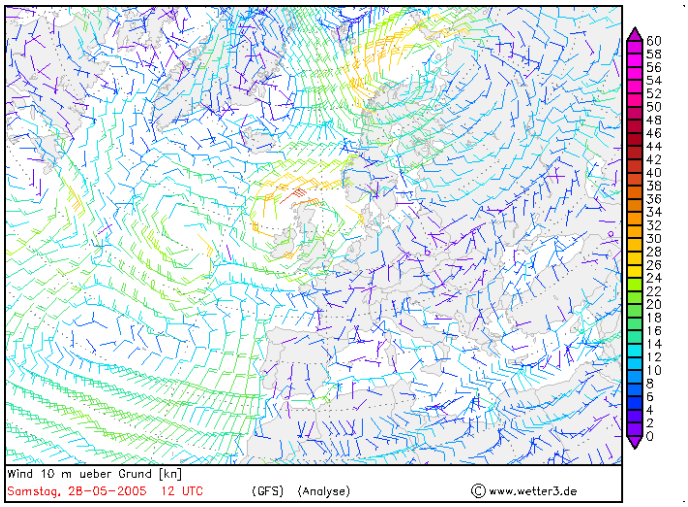

FIGURE 5.2 c) Wind speeds [knots] 10 meter above the ground at 12 UTC May 28th, 2005.

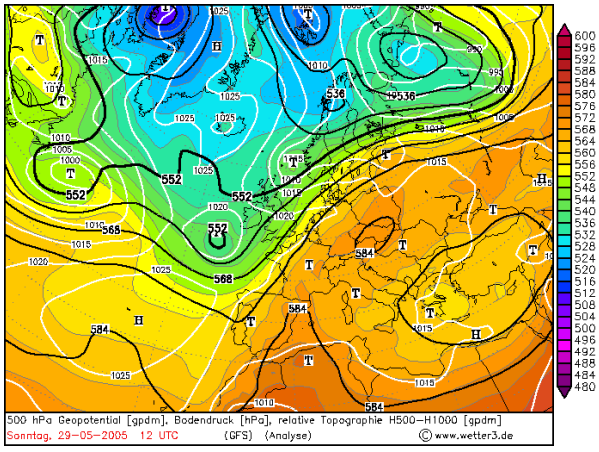

FIGURE 5.3 a) Mean sea level pressure [hPa] (white lines) at 12 UTC May 29th, 2005.

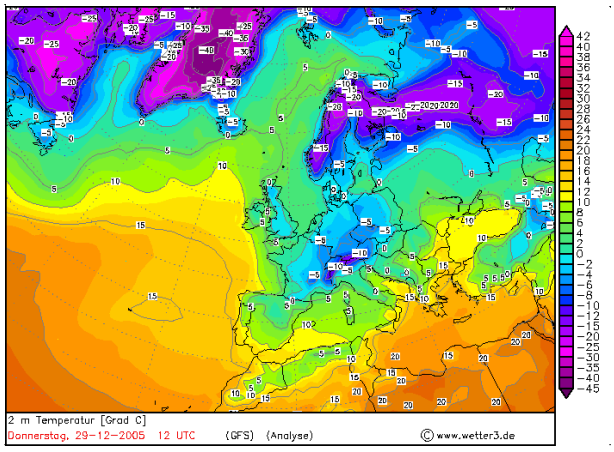

FIGURE 5.3 b) Temperature [°C] 2 meters above the ground at 12 UTC May 29th, 2005.

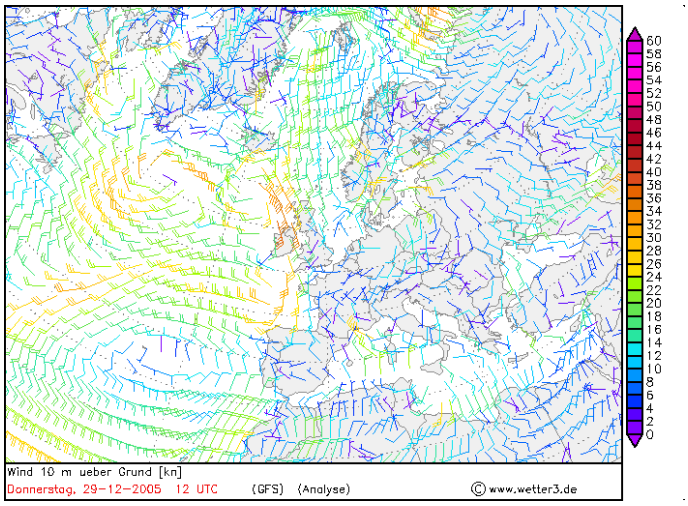

FIGURE 5.3 c) Wind speeds [knots] 10 meter above the ground at 12 UTC May 29th, 2005.

A low pressure system is centred almost directly over Ireland at the beginning of May 28th, 2005 (FIGURE 5.2a). During the day this low pressure system moves north over Ireland and dominates the weather situation in the area where sea salt aerosol production is to be studied. A weather situation dominated by a low pressure system is generally a good condition when searching for a situation with high wind speeds and considerable vertical mixing of air. As can be seen in FIGURE 5.2 c) the winds over Ireland are high during May 28th. The wind is westerly, which enhances a significant transport of sea salt to the west coast of Ireland and Mace Head from the Atlantic Ocean. As the centre of the low pressure system leaves Ireland and travel north, the wind speed, in the region to be examined, decreases. The temperature at 12 UTC this day is illustrated by FIGURE 5.2 b). During the beginning of May 28th the temperature is about 10 °C, but decreases, as the low pressure system passes over Ireland, to about 5 °C. The temperature stays low until shortly after 06 UTC May 29th. As can be seen in FIGURE 5.3 b) the temperature then increases again to a little bit warmer than 10 °C during May 29th and decreases during the evening and night with a few degrees. Another low pressure system Southwest of Ireland moves in an easterly direction during May 29th (FIGURE 5.3 a), but does not come as close to Ireland as the system the day before and therefore does not dominate the weather situation in the area of the model domain as significantly. During the period of these two days the maximum wind speeds occur between 06 and 18 UTC May 28th with wind speeds up to about 30 knots (~15 ms^{-1}). The wind speed is low in the chosen model area during the whole day of May 29th with a minimum measured wind speed at the 10-m level of about 5 knots (~2.5 ms^{-1}) which is a wind speed to low for any production of sea salt.

5.1 Horizontal Distribution

The horizontal simulated distribution of sea salt particles will in this section be studied as function of the weather situation. The mass and number concentration will be discussed in separate subsections.

5.1.1 Mass Concentration

The horizontal distribution of the mass concentration of sea salt particles and wind speed, both at a height of about 30 m above the ground, are illustrated between 6 UTC the 28th and 18 UTC the 29th in FIGURE 5.4. The concentration is always set to be zero at the boundary of the model. The mass concentration of sea salt particles is high on May 28th because of high wind speeds near the centre of the low pressure system that can be seen passing very close to, or even over, Ireland. In the centre of the low pressure system, the wind speed is not particularly high and in this area the mass concentration is also low. That low mass concentration is seen in this area is also an effect of the zero concentration boundary conditions, because the low concentrations near the border of the model domain is transported into the centre of the low pressure system. Maximum mass concentration is about 300 μg m^{-3} at mid-day May 28th. It is seen that the transport of sea salt particles over Ireland is significant but the deposition to land is also significant as the mass concentration decreases rapidly. In the evening of May 28th, when the low pressure system has moved north and the wind speeds are decreasing, the mass concentration of sea salt also decreases clearly. During the next day the weather situation is completely different with much lower wind speeds and the production of sea salt particles is also very low, especially in comparison to the previous day. The maximum mass concentration of sea salt particles during May 29th is only about 70 μg m^{-3}. The mass concentration and wind speed is clearly correlated. A relation between changes in mass concentration and temperature changes is however more difficult to see, and is further more not expected since the temperature only can influence the flux of the smallest particles and they are not influencing the total mass concentration significantly. The ground level temperature at 00 and 12 UTC May 28th and 29th are shown in FIGURE 5.5, where it is obvious that the changes in sea surface temperature are minor. The sea surface temperature is almost constant during this period of time with a temperature of about 15 °C.

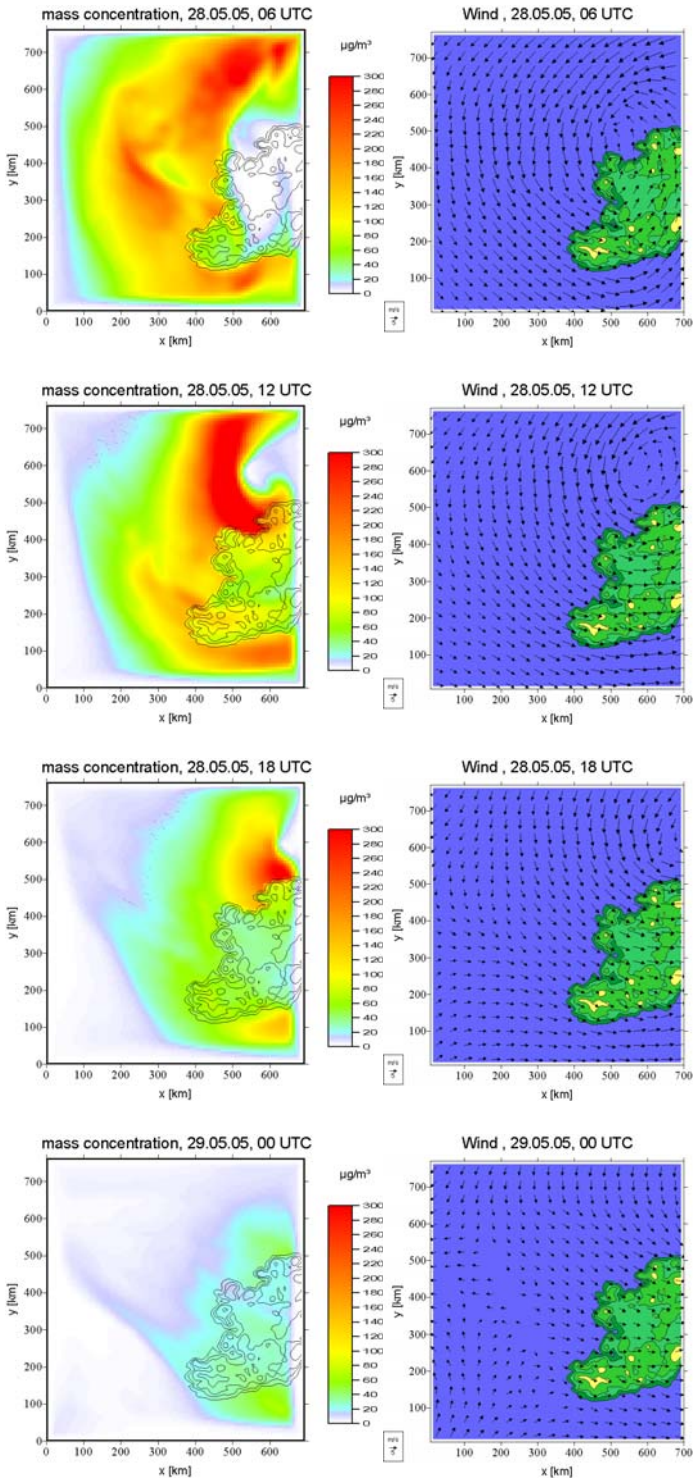

FIGURE 5.4. Mass concentration [µg m^{-3}] of sea salt particles and wind speed [m s^{-1}] every six hours between 6UTC May 28th and 18 UTC May 29th, 2005.

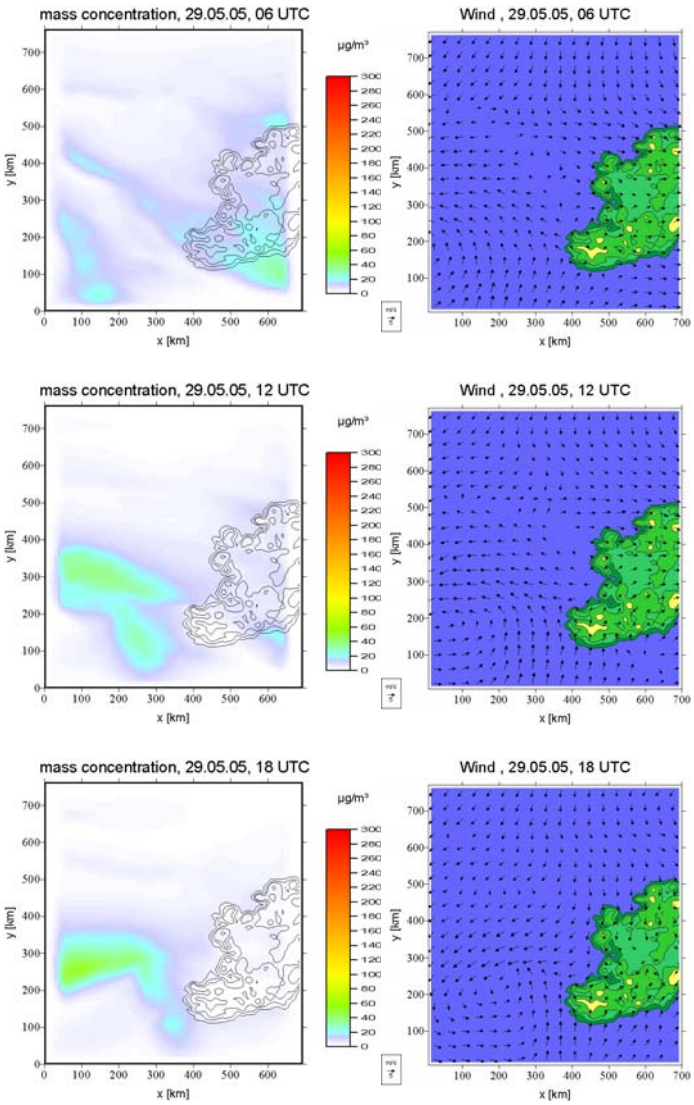

FIGURE 5.4. Continued.

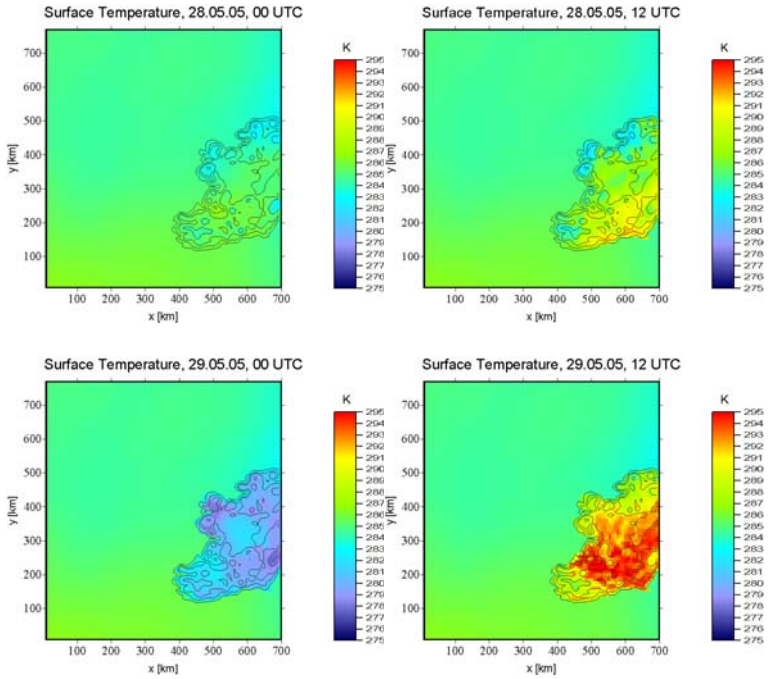

FIGURE 5.5. Surface temperature [K] at 00 and 12 UTC May 28th and 29th, 2005.

In conclusion, the influence of the wind speed is more important than the sea surface temperature for changes in mass concentration of sea salt particles and both the transport over land and the deposition to land is significant.

5.1.2 Number Concentration

The simulated number concentration and the wind speed for the period May 28-29th, 2005 are illustrated in FIGURE 5.6. As for the mass concentration is the concentration set to be zero at the boundary of the model domain, since possible transport of particles from areas outside the model area not is taken into account. The mass concentration of sea salt particles could in the last section be seen to vary greatly with wind speed, and in FIGURE 5.6 the correlation between wind speed and number concentration is also obvious. The number concentration of particles increases rapidly with time over the ocean and the particles are then very efficiently transported eastward over Ireland. The decrease over land is not as significant as could be seen for the mass concentration of sea salt particles in the last section. The number concentration is, as concluded earlier, dominated by the mode of the smallest particles whilst the mass concentration is dominated by the largest particles. Comparing number and mass concentration of sea salt particles over land it is concluded that the smallest particles dominate

over the larger particles in this area. The number concentration is large over land as well as over the ocean, i.e. the transport is important and the deposition is not as significant as for the larger particles. The simulation starts at 00 UTC the 28th and already after 3 hours the number concentration is up to 100 cm^{-3} over small areas over the ocean. The most significant transport in over the west and south coast of Ireland starts after about 5 hours. Between 10 UTC and 13 UTC the number concentration of particles over almost the whole Ireland is 100 cm^{-3}. As the low pressure system moves north the wind speed in the region decreases and the production of particles does for this reason also decrease, i.e. the amount of particles available for transport decreases and after 13 UTC the number concentration over land decreases accordingly with time. The number concentration is however at least 30 cm^{-3} over land until 3 UTC May 29th. During the afternoon and evening of 29th the wind speed increases a little over the ocean south west of Ireland and an increase in the number concentration can be seen. Any transport of particles to Ireland is however not possible since the winds mainly have the direction north-south in this area during this period of time. As mentioned in the previous section, the sea surface temperature is almost constant during the time period of simulation (FIGURE 5.5). Therefore, no conclusions can be made about the dependence of changes in number concentration with changes in sea surface temperature. As could be seen earlier the flux of particles for a sea surface temperature of 15 °C is dominated by the sub micrometer range, with a maximum flux for particles with dry particle diameter of 0.7 μm .

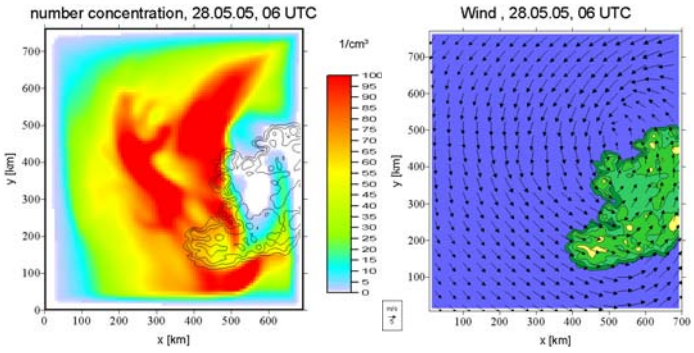

FIGURE 5.6. Number concentration [cm^{-3}] of sea salt particles and wind speed [m s^{-1}]

every six hours between 6 UTC May 28th and 18 UTC May 29th, 2005.

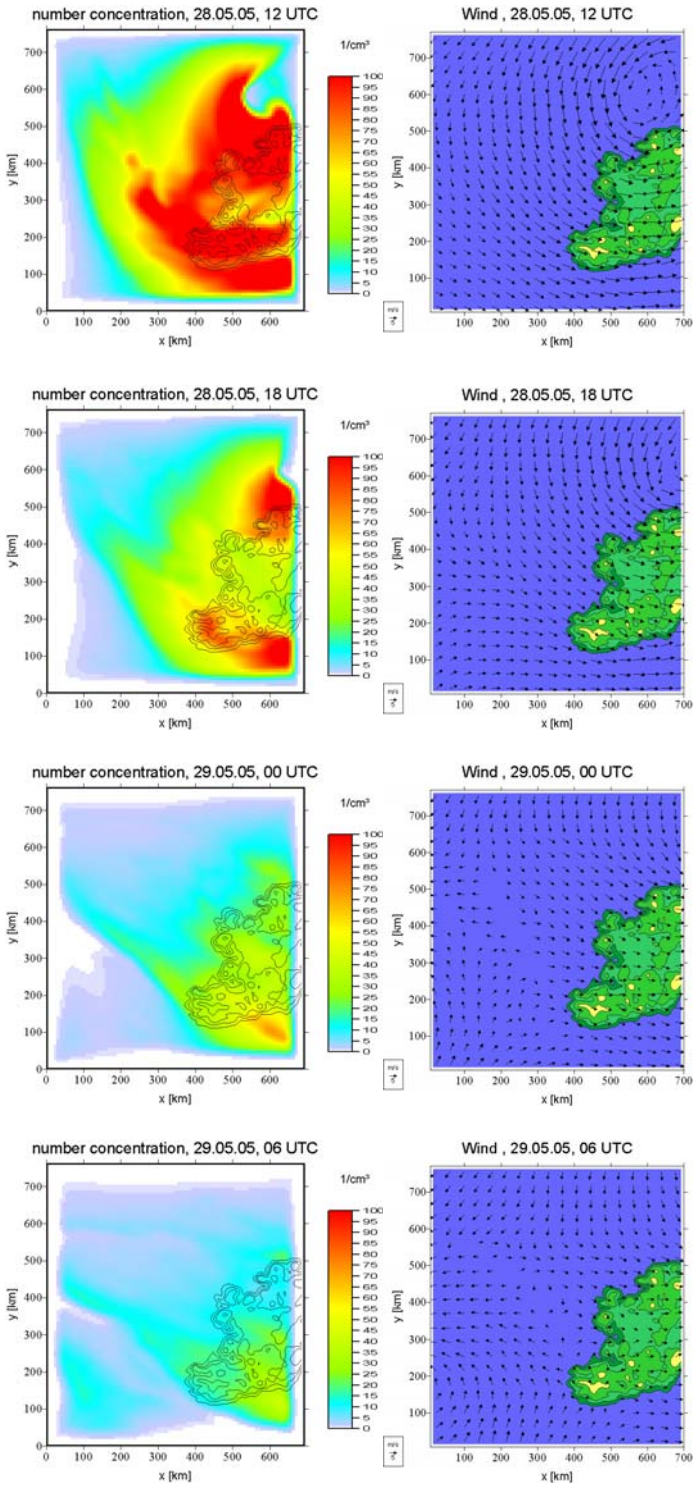

FIGURE 5.6. Continued.

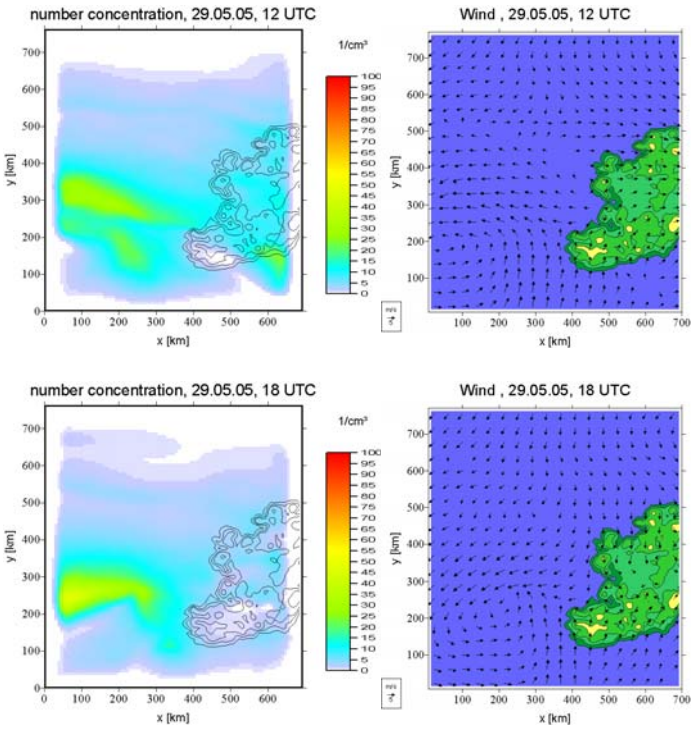

FIGURE 5.6. Continued.

5.2 Modelled Concentrations at Mace Head, Ireland.

The position of Mace Head is illustrated in FIGURE 5.7. The simulated daily cycles of the number and mass concentration of sea salt particles in Mace Head during May 28th and 29th are illustrated in FIGURE 5.8.

FIGURE 5.7. Mace Head, (53,19 N; 9,54 W),

on Ireland.

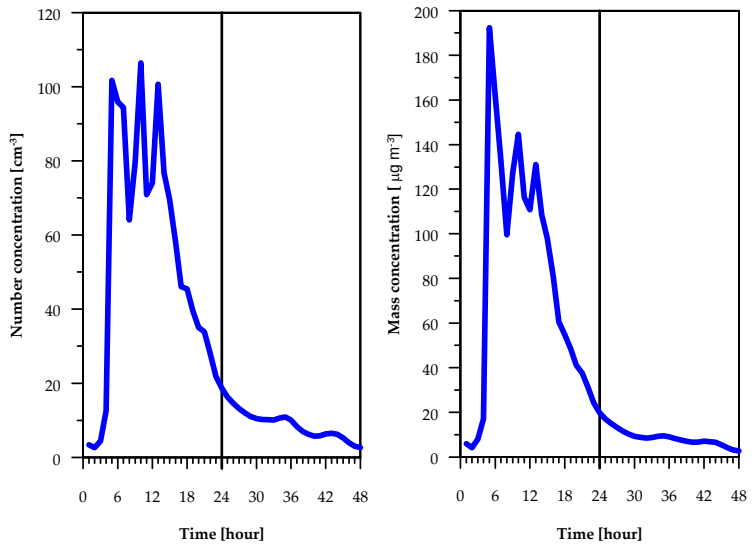

FIGURE 5.8. The change in number concentration [cm^{-3}] and mass concentration [$\mu g m^{-3}$] with time at Mace Head.

The transport of sea salt particles from the Atlantic Ocean is clearly displayed in FIGURE 5.8. The transport of particles is most effective between about 6 UTC and 14 UTC the 28th, when also the wind speed over the ocean is high and directed from the ocean towards Mace Head. Maximum mass concentration occurs at approximately 6 UTC with a concentration of 195 µg m^{-3} and then there are two smaller local maxima with number concentrations above 100 cm^{-3}. The number concentration in Mace Head do not decrease as fast as the mass concentration with time, but the maximum values of both quantities occurs at the same time.

Since in situ measured concentrations of sea salt particles are hard to find in the literature no direct comparisons between measurements and the simulated number and mass concentrations in this work can be done. The maximum number concentration of 100 cm^{-3}, both over the ocean and in Mace Head, and the maximum mass concentration of 195 µg m^{-3} in Mace Head and 300 µg m^{-3} are found in the simulations within the frames of this work. Measurements made by O'Dowd *et al*. [1997] indicate sea salt CCN concentrations as high as 100 cm^{-3} at surface wind speeds of 20 m s^{-1}. In the same paper it is described that sea salt aerosols with concentrations greater than 70 cm^{-3} at wind speeds of 17 m s^{-1} are found to dominate the accumulation aerosol mode (*film mode*) under clean marine conditions. Glantz *et al*. [2004] found number concentrations of about 100 cm^{-3} near the ground for particles smaller than 6 µm. Grini *et al*. [2002] present a 5 year average mass concentration of between 2.5 and 10 µg(Na) m^{-3} in Mace Head. O'Dowd *et al.* 2004 gave the absolute mass concentrations of sea salt for periods of low

biological activity (winter) and high biological activity (spring to autumn) up to 10 μg m^{-3} for the largest particles (FIGURE 5.9).

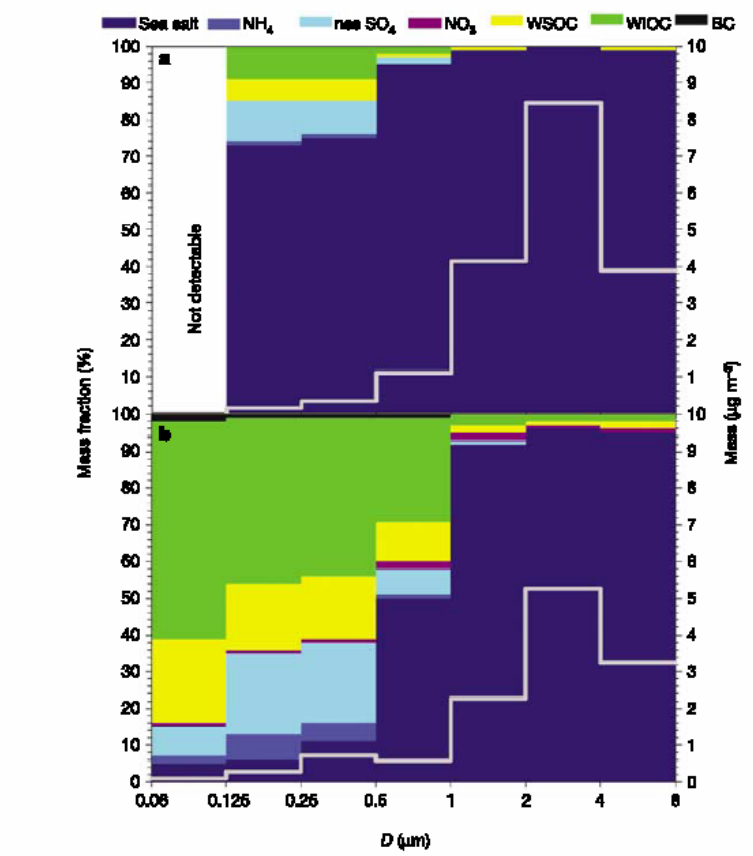

FIGURE 5.9. Average size-segregated chemical compositions and absolute mass concentrations of North Atlantic marine aerosols, shown for low biological activity period (a) and high biological activity period (b). (O'Dowd *et al*. [2004]).

In this work the concentration of sea salt particles is investigated for a stormy weather situation why the results cannot be compared results from global long time averaged simulations or measurements. Glantz *et al*. [2004] presented total sea salt mass concentration between 50 and 100 μg m^{-3} for the lowest 10 meters above the ground. The mass concentration in this work is shown at an altitude of about 30 meters, which then shall be compared to a mass concentration of about 20 μg m^{-3} in Glantz *et al*. [2004].

The given number concentrations for sea salt aerosols found in the literature are never given for the whole size interval investigated in this work, but it is seen that the simulated concentrations are in a reasonable order of magnitude compared to earlier results. In Section 3.2 it was concluded that the mass flux of sea salt particles from the sea surface to the atmosphere increases exponentially with increasing wind speed. It is therefore impossible to compare the maximum simulated mass

concentration from this high-wind situation with long time averaged mass concentrations from earlier works.

5.3 Vertical Distribution

In this section is the vertical distribution of sea salt particles in Mace Head is discussed. Further on is a latitude-height cross section done through the centre of the low pressure system at 12 UTC May the 28th to examine the number and mass concentration of sea salt particles where the maximum wind speeds were found.

5.3.1 Vertical Profile at Mace Head.

In Section 5.1 and 5.2 it was seen that higher mass and number concentrations were found on the 28th compared to the 29th because of the weather situation. For this reason the vertical profile in Mace Head is only examined as function of time for May 28th. The vertical changes of the distribution of the number and mass concentration with time are illustrated in FIGURE 5.10.

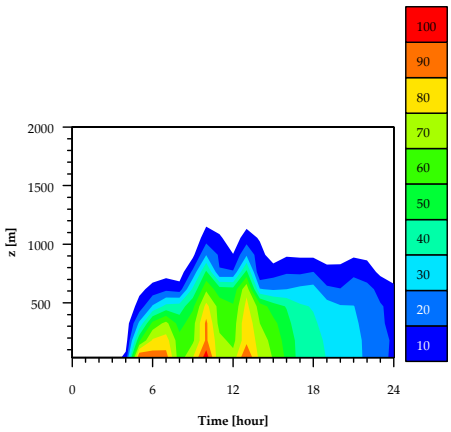

FIGURE 5.10 a Simulated daily cycle of the vertical profile of the particle number concentration [cm^{-3}] at Mace Head, at May 28th, 2005.

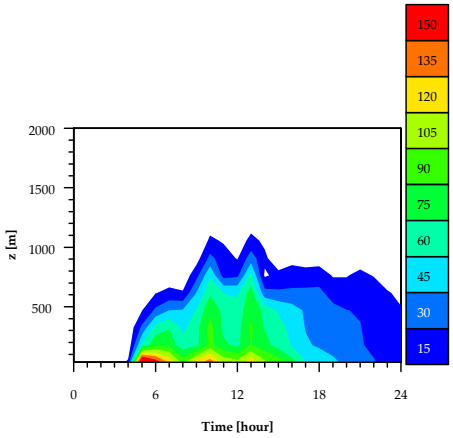

FIGURE 5.10 b Simulated daily cycle of the vertical profile of the particle mass concentration [$\mu g\ m^{-3}$] at Mace Head, at May 28th, 2005. .

The transport of sea salt particles from the Atlantic Ocean to Mace Head is again clearly seen. The transport is significant first after four hours. The vertical mixing of sea salt aerosols is substantial, especially after 6 UTC and below 700 meters height. The transport to e.g. the 500 meter level is increasing with time from 4 UTC to reach a maximum at 13 UTC, and after this point the

concentration decreases with time. The residence time in the atmosphere of sea salt particles is in general low, in the order of minutes or seconds for the largest particles and at maximum tenth of hours for the smallest particles. Comparing the number and mass concentration of sea salt particles, which are dominated in the submicrometer and super micrometer size range respectively, it is seen that the small particles stay longer in the air before sedimentation since the vertical profile of mass concentration decreases more rapidly with time than the number concentration. It is also obvious that the maximum emitted small particles also reach higher levels in the troposphere than the larger particles.

The maximum height reached by sea salt particles over Mace Head was 1.1 km and occurs two times, at 10 UTC and 13 UTC. This is clearly seen both for number and mass concentration. Local maxima in number concentration, of about 100 cm^{-3}, is again seen to occur at three occasions: between 5 and 7 UTC, at 10 UTC and at 13 UTC while the absolute maximum in mass concentration, 150 μgm^{-3}, is only seen to coincide with the two first number concentration maxima.

5.3.2 Latitude-Height Cross Section.

The maximum mass and number concentrations coincide with maximum wind speeds, which occur at 12 UTC May 28th close to the centre of the low pressure system north of Ireland (FIGURE 5.11). A vertical cross section is for this reason made through the centre of the maximum mass and number concentration of sea salt particles along y=600 km. The cross section for the number concentration is illustrated in FIGURE 5.12 and the cross section for the mass concentration is shown in FIGURE 5.13.

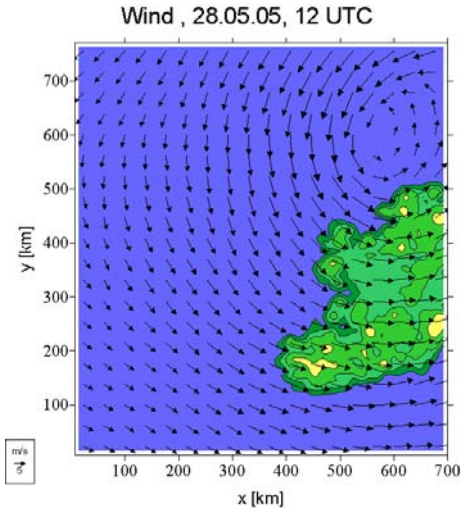

FIGURE 5.11 Wind speed [m s^{-1}] at 12 UTC, May 28th.

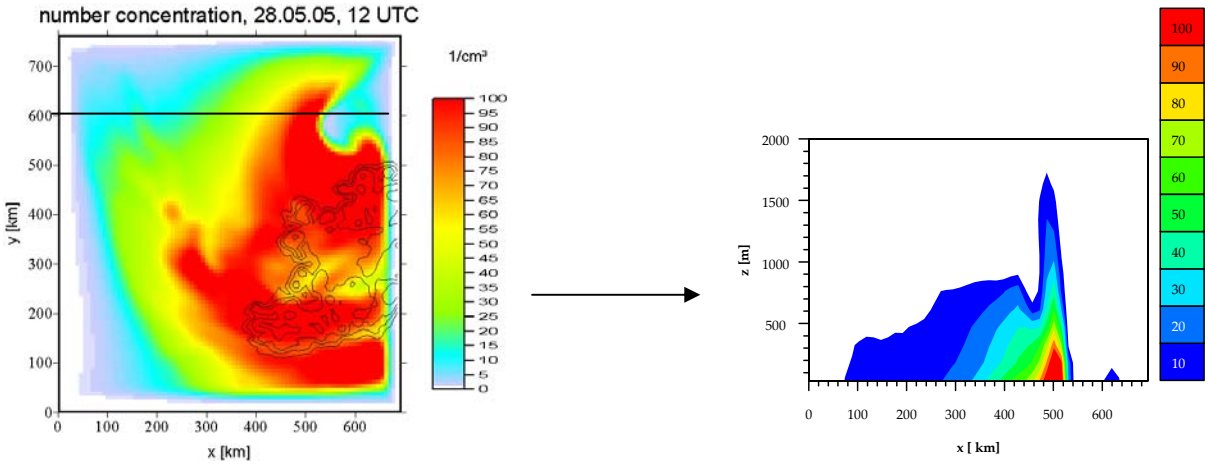

FIGURE 5.12 Vertical cross section of the particle number concentration [cm^{-3}] at y = 600 km at 12 UTC May 28th, 2005.

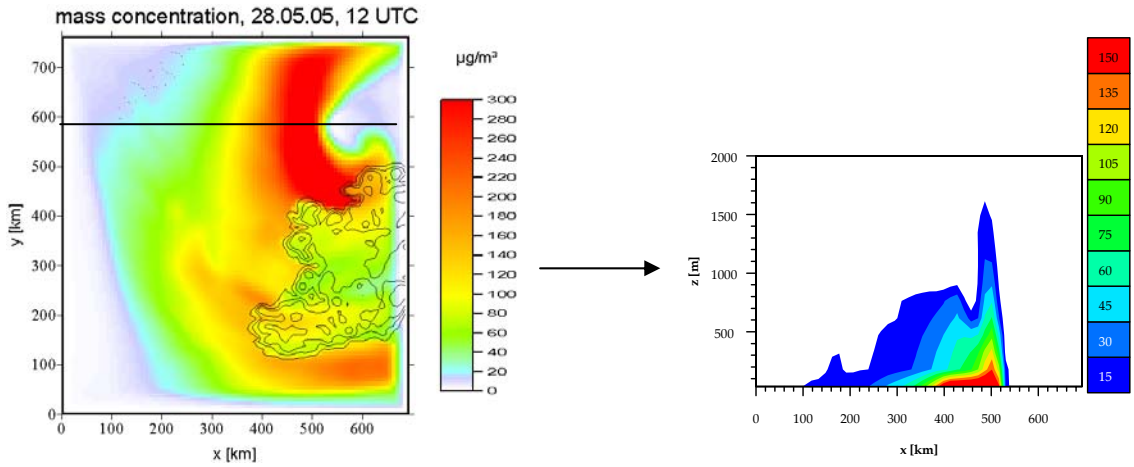

FIGURE 5.13 Vertical cross section of the particle mass concentration [$\mu g\ m^{-3}$] at y = 600 km at 12 UTC May 28th, 2005.

The vertical mixing of sea salt particles is most effective close to the centre of the low pressure system, where heights of more than 1600 m are reached. The concentrations are, as expected, decreasing with height. The number concentration decreases more slowly with altitude than the mass concentration, which indicates that more sub micrometer sized particles are transported to higher altitudes than the super micrometer sized particles. Moving away from the centre of the low pressure system the wind speed decreases and so do also the number and mass concentration of sea salt particles. Also the vertical mixing decreases when moving away from the central parts of the low pressure system.

6. Summary

The main focus of this work has been to introduce emissions of sea salt particles from the sea surface to the atmosphere into a 3-D regional atmospheric model and to study the distribution of these particles as a function of sea surface temperature and wind speed. Sea salt particles are for simplification assumed to be emitted as dry particles and it is assumed that they remain in that state during the whole model simulation. The particles are emitted in dry diameter sizes from 0.02 μm to 28 μm using a combination of three different parameterizations for the number flux of sea salt particles: Mårtensson *et al*. [2003], Monahan *et al*. [1986] and Smith *et al*. [1993]. All three parameterizations are dependent on wind speed and the parameterization of Mårtensson *et al*. [2003] is also dependent on sea surface temperature. The mass flux is then calculated from the total amount of emitted particles.

The amount of particles is concluded to increase with increasing wind speed for all three parameterizations. Changes at low wind speed convey to changes in the number concentration of the particles more quickly than changes at high wind speed. The amount of particles emitted is for all wind speeds highest for the smallest particles (sub micrometer sizes) and smallest for the biggest particles (super micrometer sizes). The number density flux of the smallest particles with diameter D_P<0.1 μm increases with decreasing temperature while the number density flux for particles with D_P>0.4 μm decreases with decreasing temperature. Between 0.1 μm and 0.4 μm no clear trend can be seen with changes in water temperature. It is concluded that the sub micrometer size range dominates the number of particles while the super size particles influences the mass concentration the most. The dependence of the mass density flux on the wind speed is exponential. The agreement is good between a calculated average annual global mass flux of 3200 Tg per year and a corresponding measured flux of 3340 Tg per year according to IPPC (2001).

3-D simulations of the sea salt aerosol mass and number concentration were made over the Atlantic Ocean for a model domain west of Ireland for the period of 28th to 29th of May, 2005. The concentration of emitted sea salt particles is found to depend highly on the wind speed and reached a maximum mass concentration of 300 μg m^{-3} over the ocean in combination with wind speeds of 15 m s^{-1}. The maximum number concentration of 100 cm^{-3} is found both over ocean and over land. It would have been interesting to compare this result with corresponding in situ measurements of sea salt concentrations. This comparison is however not possible, as measurements for the simulated time period are not available. In comparison to earlier simulations and measurements, where CCN number

concentration of 100 cm^{-3} is found for high wind speeds (20 m s^{-1}) (O'Dowd *et al*. [1997]) and number concentrations for particles with D_P<0.7 μm are found in the order of 100 cm^{-3} (Glantz et al. [2004]), it is concluded that the particle number concentrations are of reasonable order of magnitude. For the mass concentration, comparisons with earlier results are more difficult to perform. Global simulations and measurements averaged over periods of months have given mass concentrations up to 10 μg m^{-3} in Mace Head (O'Dowd *et al*. [2004], Grini *et al*. [2002]). Glantz *et al.* [2004] presented a total sea salt particle mass of 100 μg m^{-3} at ground level, which is of the same order of magnitude as the results in this work. The results in this work are however presented at a higher altitude, where Glantz *et al*. [2004] found mass concentrations of the order of 20 μg m^{-3}. Since the maximum simulated sea salt mass concentration of 300 μg m^{-3} over the ocean and the maximum concentration of 190 μg m^{-3} in Mace Head are found for a weather situation with high wind speeds, these results cannot be compared to results averaged over long time periods. It is concluded that the values of simulated number concentration are reasonable and that the mass concentration can not really be compared with any similar situations.

The transport of sea salt particles to areas where no sea salt particles can be produced is found to be substantial. The number concentrations 100 cm^{-3} of sea salt aerosols found over the ocean are also found over land, whereas the mass concentration decreases rapidly over land. The maximum mass concentration transported over land is of the order of 90 μg m^{-3}. No comparable measurements have been found over land but the conclusion that small concentrations are found over land was for example done by Grini *et al*. [2002]. They simulated a maximum mass concentration of 4 μg m^{-3} over land in comparison to 10 μg m^{-3} over the ocean.

The transport over land and the vertical mixing is found to be most effective for the smallest particles, since the number concentration decreases more slowly than the mass concentration over land and with height. The sea salt particles are transported to a maximum height of about 1.1 km over Mace Head and 1.6 km over the ocean in the area where the strongest wind speeds are found for this period. Grini *et al*. [2002] concluded that the vertical transport of sea salt particles is small and that no significant amount of particles could be found above the 750 hPa level, which coincides with the results from this study. In the paper of Glantz *et al*. [2004] the maximum reached altitude for the sea salt aerosols was 0.9 km.

No dependence of the number or mass concentration on temperature could be noticed because of the almost non-existent variation in sea surface temperature during the simulation period. To be able to study the sea surface temperature effect on the sea salt aerosol production a longer time period has to be chosen. In this work it has been noticed that the total amount of particles emitted from the sea surface to the atmosphere increases with decreasing temperature for a certain wind speed. A number concentration should therefore be larger during a winter period than a summer period, for instance. This was seen in the paper of Grini *et al*. [2002] where the production was found to be larger at winter latitudes than at summer latitudes. The global maximum sea salt aerosol production (about 420 mg m^{-2} day^{-1}) was in this paper found near Ireland in January, while the production over the same area was not as significant in July (about 110 mg m^{-2} day^{-1}).

In this work the sea salt particles were assumed to be emitted to the atmosphere as dry particles and to remain dry during transport. In future work this simplification will be abandoned and chemistry between sea salt particles and the surroundings will be introduced. An accurate description of the sea salt aerosols with sizes changing with ambient relative humidity is important when examining feedback processes of the particles. For instance are the effects from particles scattering incoming sunlight, forming cloud condensation nuclei's and providing media for heterogeneous chemistry in the atmosphere depending on the sizes of the particles. Small particles are more important in scattering light processes while larger particles have bigger surface area where atmospheric chemical processes can take place. Furthermore, wet deposition is not included in the frames of this work. This is an important sink for the sea salt particles, and the concentrations would have been smaller with this process included. How big effect wet deposition have on sea salt particles will be investigated in the future.

Acknowledgements

I have had the privilege to work with a great research group at the Institute of Meteorology and Climate Research at the University of Karlsruhe in Germany. I would like to start thanking you all (Bernhard Vogel, Heike Vogel, Tanja Stanelle, Rayk Rinke and Dominique Bäumer) for welcoming me so warmly and always being there for me. Biggest Thank You to Bernhard Vogel for coming up with the idea for my study, having a lot of time for me and answering my questions, reading and commenting my report- always in a professional way. I want to thank Heike Vogel and Tanja Stanelle for having time for me from day one and especially for the help with my simulations. A lot of thanks

to Annica Ekman for supporting me from Stockholm and giving me so many useful comments to my report. I also want to thank Monica Mårtensson for giving me some background to the field of sea salt particle production simulations. At last but not least I am very grateful to Prof. Dr. Christoph Kottmeier for accepting me as a student at the institute and with that making my cooperation with the group possible!

Appendix A: LM - Basic Equations

The following section describes structure of LM, with selected information extracted from the documentation by Doms and Schättler [2002]. LM has been designed for operational weather prediction (NWP) as well as scientific applications on the meso-β and the meso-γ scale. The model works over a regional area of up to 2000×2000 km², e.g. Central Europe, and to a height of 24 km. Many possible applications of different kinds convey a number of physical, numerical and technical design requirements for the model.

Since the LM is an atmospheric simulation model at the very high spatial solution of 7 km, or even less, the hydrostatic approximation has to be abandoned and a non-hydrostatic equation system is required. The pressure is calculated from a 3-D prognostic equation derived from the complete continuity equation and the temperature equation (Steppler *et al*. [2002]).

LM is based on thermo-hydro-dynamical equations describing a compressible moist model atmosphere. As horizontal coordinate system the spherical coordinate's latitude and longitude are used. Spherical coordinates are not defined at the poles, but since the LM is not used globally, the coordinate system is shifted so that the poles always are outside of the model area.

When the geometrical height z above the mean sea level is used as vertical coordinate and surface terrain is included costly formulations of the lower boundary conditions give a complex numerical solution to the equations. To be able to formulate the boundary conditions on the earth's surface more easily, a generalized time independent terrain following height coordinate is used in LM. The lowest surface of constant vertical coordinate then becomes adjusted to the terrain height.

The initial version of the LM dynamical core is, as many other non-hydrostatic models, based on the HE-VI (horizontal explicit, vertical implicit) time splitting technique, which is an algorithm that combines the forward-backward time integration for horizontal wave modes with implicit time differencing for vertical modes. The result is a scheme stable with respect to vertical propagation of acoustic waves.

The atmosphere is considered as a multi-component continuum constituted by dry air, water vapour, liquid water and water in solid state. External forces as gravity- and Coriolis forces and internal processes due to heat, mass and momentum transfer and phase changes of water have impact on the system. The basic conservation laws for momentum, mass and heat are then given by the following budget equations given in advection form with Lagrangian time derivative:

$$\begin{aligned}
\rho\frac{d\vec{v}}{dt} &= -\nabla p + \rho\vec{g} - 2\vec{\Omega}\times(\rho\vec{v}) - \nabla\cdot\underline{t} \\
\frac{d\rho}{dt} &= -\rho\nabla\cdot\vec{v} \\
\rho\frac{dq^x}{dt} &= -\nabla\cdot J^x + I^x \\
\rho\frac{de}{dt} &= -p\nabla\cdot\vec{v} - \nabla\cdot(J_e + R) + \varepsilon
\end{aligned} \qquad \text{(A1)}$$

x represents dry air (x=d), water vapour (x=v), liquid water (x=l) or water in frozen state (x=f).

$\vec{v}$: barycentric velocity (relative to the rotating earth)

p : pressure

ρ : total density of the air mixture

e : specific internal energy

$\vec{\Omega}$:constant angular velocity of earth rotation

$\underline{t}$: stress tensor due to viscosity

J_e : diffusion flux of internal energy (heat flux)

J^x : diffusion flux of constituent x

I^x : sources/sinks of constituent x

q^x :mass fraction of constituent x $\left(=\frac{\rho^x}{\rho}\right)$

R : flux density of solar and thermal radiation

$\vec{g}$: gravity acceleration

ε : kinetic energy dissipation due to viscosity

$\frac{d}{dt}$: total Lagrangian time derivative operator, $\frac{d}{dt}=\frac{\partial}{\partial t}+\vec{v}\cdot\nabla$ where $\frac{\partial}{\partial t}$ is local Eulerian time derivative operator.

∇ : gradient Nabla operator

In order to get the final equations of LM a decomposition of the variables using Reynolds averaging and mass weighted averages are applied to equations (A1) using the following decompositions:

$$\Psi = \overline{\Psi} + \Psi' \text{ with } \overline{\Psi'} = 0 \tag{A2}$$

and

$$\Psi = \hat{\Psi} + \Psi'' \text{ with } \hat{\Psi}'' = 0 \tag{A3}$$

where the following average is used:

$$\hat{\Psi} = \overline{\rho\Psi} / \overline{\rho} \,. \tag{A4}$$

With these conventions and several simplifications with respect to the thermodynamics Reynolds averaging of the equations is applied. When omitting the hat and the bar symbols one ends with the following set of equations:

$$
\begin{aligned}
\rho\frac{d\vec{v}}{dt} &= -\nabla p + \rho\vec{g} - 2\vec{\Omega}\times(\rho\vec{v}) - \nabla\cdot\underline{T} \\
\frac{dp}{dt} &= -\left(\frac{c_{pd}}{c_{vd}}\right)p\nabla\cdot\vec{v} + \left(\frac{c_{pd}}{c_{vd}} - 1\right)Q_h \\
\rho c_p\frac{dT}{dt} &= \frac{dp}{dt} + Q_h \\
\rho\frac{dq^v}{dt} &= -\nabla\cdot F^v + \left(I^l + I^f\right) \\
\rho\frac{dq^{l,f}}{dt} &= -\nabla\cdot\left(P^{l,f} + F^{l,f}\right) + I^{l,f} \\
\rho &= p\left[R_d\left(1 + (R_v/R_d - 1)q^v - q^l - q^f\right)T\right]^{-1}
\end{aligned}
\tag{A5}
$$

T is the temperature and Q_h represents the diabatic heating due to condensation and freezing and the divergence of the heat and the radiative fluxes, respectively. c_{vd} is the specific heat of dry air at constant volume and c_{pd} is in the same way the specific heat at constant pressure. R_d and R_v are, respectively, the gas constant for dry air and water vapour. P^l represents the precipitation flux of water and P^f the precipitation flux of ice.

The turbulent fluxes of momentum

$$\underline{T} = \overline{\rho v'' v''} \tag{A6}$$

and of any other scalar x

$$F^x = \overline{\rho v'' x''} \tag{A7}$$

are parameterized as described in Doms and Schättler [2002]. All equations are finally transferred into spherical and terrain following coordinates. After discretization the equations are integrated numerically.

Bibliography

Andreas, E. L., 1998: "A new Sea Spray Generation Function for Wind Speeds up to 32 m s^{-1}", *Journal of Physical Oceanography 28,* pp. 2175-2184.

Archer, C. L. and M. Z. Jacobson, 2005: "Evaluation of global wind power", *Journal of Geophysical Research 110,* 20 pp.

Binowski, F. S. and U. Shankar, 1995: "The regional particulate matter model, 1. Model description and preliminary results", *Journal of Geophysical Research 100(D12),* pp. 26191-26209.

Clarke, A., V. Kapustin, S. Howell and K. Moore, 2003: "Sea-Salt Distributions from Breaking Waves: Implications for marine Aerosol Production and Optical Extinction Measurements during SEAS*", *Journal of Atmospheric and Oceanic Technology 20(D12110),* pp. 1362-1374.

Doms, G. and U. Schättler, 2002: "A description of the Nonhydrostatic Regional Model LM", Deutscher Wetterdienst, P. O. Box 100465, 63004 Offenbach, Germany. (http://www.cosmo-model.org).

Erickson, D. J. and R. A. Duce, 1988: "On the global flux of atmospheric sea salt", *Journal of Geophysical Research 93,* pp. 14079-14088.

Finlayson-Pitts, B. J. and J. C. Hemminger, 2000: "Physical Chemistry of Airborn Sea Salt Particles and Their Components", *Journal of Physical Chemistry 104(49),* pp. 11463-11477.

Foltescu, V. L., S. C. Pryor and C. Bennet, 2005: "Sea salt generation, dispersion and removal on the regional scale", *Atmospheric Environment 39,* pp. 2123-2133.

Gong, S. L. and L. A. Barrie, 1997: "Modeling sea-salt aerosols in the atmosphere, 1. Model development", *Journal of Geophysical Research 102(D3),* pp. 3805-3818.

Glantz, P., G. Svensson, K. J. Noone and S. R. Osborne, 2004: " Sea-salt aerosols over north-east Atlantic: Model simulations of the ACE-2 Second Lagrangian experiment", *Q. J. R. Meteorological Society 130*, pp. 2191-2215.

Grini, A., G. Myhre, J. K. Sundet and I. S. A. Isaksen, 2002: "Modeling the Annual Cycle of Sea Salt in the Global 3D Model Oslo CTM2: Concentrations, Fluxes and Radiative Impact", *Journal of Climate 15*, pp. 1717-1730.

Hoppel, W. A., G. M. Frick and J. W. Fitzgerald, 2002: "Surface source function for sea-salt aerosol and aerosol dry deposition to the ocean surface", *Journal of Geophysical Research 107(d19)*, pp. 4382-4398.

IPPC, 2001: Contribution of the Working Group I to the Third Assessment Report of the Intergovernmental Panel on Climate Change (IPCC). In J. T. Houghton, Y. Ding, D. J. Griggs, M. Noguer, P. J. van der Linden and D. Xiaosu (Eds.), "Climate Change 2001: The Scientific Basis". *Cambridge University Press, UK.*

Lewis, E. R. and S. E. Schwartz, 2006: "Comment on „size distribution of sea-salt emissions as a function of relative humidity"", *Atmospheric Environment 40*, pp. 588-590.

Kramm, G., K. D. Beheng and H. Müller, 1992: "Modeling of the vertical transport of polydispersed aerosol particles in the atmosphere surface layer" in Stephen E. Schwartz, Hrsg. "Precipitation Scavenging and Atmosphere-Surface Exchange", Bd.2:*The Richard G. Semonin volume, Hemisphere Publ., Washington,* pp. 1125-1141.

Mårtensson,E.M., D. Nilsson, G. De Leeuw, L.H. Cohen and H.-C. Hansson, 2003: "Laboratory simulations and parameterization of the primary marine aerosol production", *Journal of Geophysical Research 108(D)*, pp. 4297-4308.

Monahan, E. C. and I. O'Muircheartaigh, 1980: "Optimal Power-Law Description of Oceanic Whitecap Coverage Dependece on Wind Speed", *Journal of Physical Oceanography 10,* pp. 2094-2099.

Monahan, E. C. C. W. Fairall, K. L. Davidson and P. Jones Boyle, 1983: "Observed inter-relations between 10 m winds, ocean whitecaps and marine aerosols", *Q. J. R. Meteorological Society 109,* pp. 379-392.

Monhanan, E. C, D. E. Spiel and K. L. Davidson, 1986: "A model of marine aerosol generation via whitecaps and wave disruption" in *Oceanic Whitecaps,* edited by E. C. Monahan and G. Mac Niocaill, *D. Reidel publishing Company,* pp. 167-174.

O'Dowd, C. D., and M. H. Smith, 1993: "Physiochemical properties of aerosols over the Northeast Atlantic: Evidence for wind speed related submicron sea salt aerosol production", *Journal of Geophysical Research 98,* pp. 1137-1149.

O'Dowd, C. D., M. H. Smith, I. E. Consterdine and J. A. Lowe, 1997: "Marine aerosol, sea-salt, and the marine sulpur cycle: A short review", *Atmospheric Environment 31*, pp. 73-80.

O'Dowd, C. D., M. C. Facchini, F. Cavalli, D. Ceburnis, M. Mircea, S. Decesari, S. Fuzzi, Y. J. Yoon and J.-P. Putaud, 2004: "Biogenically driven organic contribution to marine aerosol", *Nature* 431, pp. 676-680.

Riemer, N., H. Vogel, B. Vogel and F. Fiedler, 2003: "Modeling aerosols on the mesoscale-γ: treatment of soot aerosol and its radiative effects", *Journal of Geophysical Research 108(D19),* 4601.

Satheesh, S. K., K. Krishna Moorthy, 2005: "Radiative effects of natural aerosols: A review", *Atmospheric Environment 39*, pp. 2089-2110.

Seinfeld, J. H. and S. N. Pandis, 1998: "Atmospheric Chemistry and Physics, From Air Pollution to Climate Change", *John Wiley and sons,* 1326 pp.

Smith, M. H., P. M. Park and I. E. Consterdine, 1993: "Marine aerosol concentrations and estimated fluxes over the sea", *Q. J. R. Meteorological Society 119*, pp. 809-824.

Spiel, D. E., 1998: "On the birth of film drops from bubbles bursting on seawater surfaces", *Journal of Geophysical Research 95*, pp. 18,281-18,288.